



# Tristable Phenomenon in a Predator–Prey System Arising from Multiple Limit Cycles Bifurcation

Jiao Jiang

*Department of Mathematics, Shanghai Maritime University,  
Shanghai 201306, P. R. China  
jiaojiang@shmtu.edu.cn*

Wenjing Zhang

*Department of Mathematics and Statistics,  
Texas Tech University, Texas 79409, USA  
wenjing.zhang@ttu.edu*

Pei Yu\*

*Department of Applied Mathematics, Western University,  
London, Ontario N6A 5B7, Canada  
pyu@uwo.ca*

Received May 23, 2019; Revised September 22, 2019

In this paper, we consider a predator–prey system with Holling type III ratio-dependent functional response. Such a system can exhibit complex dynamical behavior such as bistable and tristable phenomena which contain equilibria and oscillating motions for certain parameter values. In particular, we show that the ratio-dependent predator–prey system can exhibit multiple limit cycles due to Hopf bifurcation, giving rise to coexistence of stable equilibria and stable periodic solutions. These solutions may reveal some new type of patterns of complex dynamical behaviors in predator–prey systems.

*Keywords:* Predator–prey system; Holling type functional response; Hopf bifurcation; bistable, tristable; limit cycle; normal form; focus value.

## 1. Introduction

Populations cannot exist in isolation in the natural environment. Individuals of different species constantly interact in the form of four major types: competition, predation, parasitism and mutualism, which are categorized at the level where one population interacts with another. Predation is one of the most fundamental interactions and one of the most fascinating interactions to investigate. Since the first predator–prey model was proposed independently by Lotka and Volterra [Lotka, 1925; Volterra, 1926], the construction and study of models for

the population dynamics of predator–prey systems have remained a dominant branch in theoretical and mathematical ecology (e.g. see [Freedman, 1980; Murray, 2002] and references therein). A well-known generalized Gause predator–prey system [Freedman, 1980; Gause, 1969] is given by

$$\begin{aligned}\dot{x} &= rx \left(1 - \frac{x}{K}\right) - yp(x), \\ \dot{y} &= y[-d + cp(x)],\end{aligned}\tag{1}$$

where  $x(t)$  and  $y(t)$  represent the population densities of prey and predator at time  $t$ , respectively;

---

\*Author for correspondence

$r, K, c$  and  $d$  are positive constants that stand for the prey's intrinsic growth rate, the carrying capacity of the prey, the conversion rate of the prey to the predator, and the predator death rate, respectively; and  $p(x)$  is the functional response function, which reflects the capturing ability of the predator to the prey. Using different functional responses, a wide variety of models have been studied extensively in the past few decades.

The term “functional response” was first introduced in [Solomon, 1949] but has become particularly associated with the work of Holling [Holling, 1959a, 1959b] through his classification of functional responses into three basic types [Collings, 1997]: (i) Lotka–Volterra type:  $p(x) = mx$ , where  $m > 0$  is the conversion rate of predators, which is an unbounded function, found in passive predators like spiders. (ii) Holling type II or Michaelis–Menten type [Holling, 1965]:  $p(x) = \frac{mx}{a+x}$ , where  $a > 0$  is called the half-saturation constant, which is bounded, satisfying  $p'(x) > 0$  for  $x \geq 0$  and  $\lim_{x \rightarrow \infty} p(x) = m$ . (iii) Generalized Holling type III or sigmoidal [Bazykin, 1998]:  $p(x) = \frac{mx^2}{ax^2+bx+1}$ , where  $b > -2\sqrt{a}$ . When  $b = 0$ , it is called the Holling type III response function. This functional response can have different behaviors according to the sign of the parameter  $b$ . When  $b \geq 0$ , the sigmoid function  $p(x)$  is asymptotically monotonic increasing, and has been studied biologically in [Jost et al., 1973a, 1973b]. It was particularly used to model the predation of *Tetrahymena pyriformis* on *Escherichia coli* or *Azotobacter vinelandii* in a chemostat. When  $b < 0$ ,  $p(x)$  is a nonmonotonic functional response, which increases to a maximum and then decreases, approaching  $\frac{m}{a}$  as  $x$  goes to infinity, representing the phenomenon of group defence formation [Lamontagne et al., 2008; Ruan & Xiao, 2001; Taylor, 1984]. Several experiments have been carried out by Andrews [1968], Boon and Lancelout [1962] and Edwards [1970] to show that nonmonotonic responses are present at the microbial level when the nutrient (prey) concentration reaches a high level, in which case an inhibitory effect on the specific growth rate occurs [Broer et al., 2006]. The rich dynamics of the predator–prey model (1) with one of the above three types of functional responses have been studied extensively, see for example, [Seo & DeAngelis, 2011] for Holling type I, [Freedman, 1980; Bazykin, 1998; Kuang & Freedman, 1988; May, 1973] for Holling type II, and [Lamontagne et al., 2008] for generalized Holling

type III. Especially Lamontagne et al. [2008] made a complete investigation on the bifurcation of singular points including Hopf bifurcation of codimensions one and two, and Bogdanov–Takens bifurcation of codimensions two and three.

The Holling type functional response is also called prey-dependent functional response which only depends on the prey density, being independent from the total amount of predators. Later, it became well recognized that the functional response can be predator-dependent at larger time and spatial scales (e.g. see [Arditi & Saiah, 1992; Beddington, 1975; Berryman, 1992; Cosner et al., 1999; DeAngelis et al., 1975; Gutierrez, 1992; Morozov & Arashkevich, 2008]). A particularly important form of predator-dependent functional response is the ratio-dependent response proposed by Arditi and Ginzburg [1989],

$$p\left(\frac{x}{y}\right) = \frac{c\left(\frac{x}{y}\right)}{m + \frac{x}{y}} = \frac{cx}{my + x}, \quad (2)$$

where the per capita predator growth rate is a function of the ratio of the prey to the predator abundance. It has been strongly supported by numerous fields and laboratory experiments [Arditi et al., 1991; Bishop et al., 2006; Hanski, 1991; Reeve, 1997] that the prey-dependent response failed to explain the observed patterns. The dynamics of system (1) with the functional response (2) has been extensively studied to examine complex bifurcation phenomena and dynamical behaviors such as deterministic extinction, existence of multiple attractors and limit cycles. It was shown in [Berezovskaya et al., 2001; Hsu et al., 2001; Xiao & Ruan, 2001] that there exist numerous kinds of topological structure in a neighborhood of the origin, including parabolic orbit, elliptic orbits, hyperbolic orbits, and any combination of them depending on parameter values. For more studies on predator–prey systems with ratio-dependent Holling type II functional response, we refer to [Jost et al., 1999; Haque, 2009; Kuang, 1999; Li & Kuang, 2007; Kuang & Beretta, 1998; Xiao et al., 2006], and references therein.

Indeed, if the predators are more efficient at higher prey densities and less efficient at lower prey densities, then the dynamics of the ecosystem is better described by the Holling type III functional response. Therefore, a generalized Holling type III

ratio-dependent function can be written in the form of (e.g. see [Huang *et al.*, 2014])

$$p\left(\frac{x}{y}\right) = \frac{m\left(\frac{x}{y}\right)^2}{a\left(\frac{x}{y}\right)^2 + b\left(\frac{x}{y}\right) + 1} = \frac{mx^2}{ax^2 + bxy + y^2} \quad (3)$$

and then the following ratio-dependent predator–prey model is obtained,

$$\begin{aligned} \dot{x} &= rx\left(1 - \frac{x}{K}\right) - \frac{mx^2y}{ax^2 + bxy + y^2}, \\ \dot{y} &= y\left(\frac{mcx^2}{ax^2 + bxy + y^2} - d\right). \end{aligned} \quad (4)$$

When  $b = 0$ , Xu *et al.* [2009] discussed the effect of time delay due to gestation of predator on the global dynamics of system (4), and Pal *et al.* [2014] investigated the existence of the equilibria of the system having time delay, and their local and global stabilities with resource limitation of the prey logistic equation and with intra-species competition among predators. For the predator–prey systems, it is well-known that the existence of limit cycles is related to the existence and bifurcation of a positive equilibrium, homoclinic bifurcation and saddle-node bifurcation. In general, it is quite difficult to determine the number of limit cycles bifurcating from a Hopf critical point. In our previous paper [Jiang & Yu, 2017], we have investigated prey-dependent or ratio-dependent predator–prey system (1) with Holling types I, II and III functional responses. In particular, based on the combination of the different types of functional responses, we list nine systems:

$$A_i : \begin{cases} \dot{x} = rx\left(1 - \frac{x}{K}\right) - mxy, \\ \dot{y} = y(mcx - d); \end{cases} \quad (5)$$

$$A_{ii} : \begin{cases} \dot{x} = rx\left(1 - \frac{x}{K}\right) - \frac{mxy}{a + x}, \\ \dot{y} = y\left(\frac{mcx}{a + x} - d\right); \end{cases} \quad (6)$$

$$A_{iii} : \begin{cases} \dot{x} = rx\left(1 - \frac{x}{K}\right) - \frac{mx^2y}{ax^2 + bx + 1}, \\ \dot{y} = y\left(\frac{mcx^2}{ax^2 + bx + 1} - d\right); \end{cases} \quad (7)$$

$$B_i : \begin{cases} \dot{x} = rx\left(1 - \frac{x}{K}\right) - mx, \\ \dot{y} = mcx - dy; \end{cases} \quad (8)$$

$$B_{ii} : \begin{cases} \dot{x} = rx\left(1 - \frac{x}{K}\right) - \frac{mxy}{x + ay}, \\ \dot{y} = y\left(\frac{mcx}{x + ay} - d\right); \end{cases} \quad (9)$$

$$B_{iii} : \begin{cases} \dot{x} = rx\left(1 - \frac{x}{K}\right) - \frac{mx^2y}{ax^2 + bxy + y^2}, \\ \dot{y} = y\left(\frac{mcx^2}{ax^2 + bxy + y^2} - d\right); \end{cases} \quad (10)$$

$$C_i : \begin{cases} \dot{x} = rx\left(1 - \frac{x}{K}\right) - mxy, \\ \dot{y} = sy\left(1 - \frac{y}{hx}\right); \end{cases} \quad (11)$$

$$C_{ii} : \begin{cases} \dot{x} = rx\left(1 - \frac{x}{K}\right) - \frac{mxy}{a + x}, \\ \dot{y} = sy\left(1 - \frac{y}{hx}\right); \end{cases} \quad (12)$$

$$C_{iii} : \begin{cases} \dot{x} = rx\left(1 - \frac{x}{K}\right) - \frac{mx^2y}{ax^2 + bx + 1}, \\ \dot{y} = sy\left(1 - \frac{y}{hx}\right). \end{cases} \quad (13)$$

Note that in the last three systems, a negative, constant term is added to measure the rate of *harvesting* or *removal* [Xiao *et al.*, 2006] for the system, which enables one to analyze the general effect of harvesting on these models. Also note that all the parameters should take positive values, except for  $b$  which may also take zero or negative values, satisfying  $b > -2\sqrt{a}$ .

In [Jiang & Yu, 2017], we have given a complete analysis on the dynamics and bifurcations of the

systems (5)–(9) and particularly show that the  $A_{iii}$  model [system (7)] can exhibit bistable and tristable phenomena due to Hopf bifurcation, giving rise to the coexistence of stable equilibria and stable limit cycles. In this paper, we focus on the  $B_{iii}$  model [system (10)], a ratio-dependent predator–prey system with generalized Holling type III functional response and study multiple limit cycles bifurcation and their stability, giving rise to the interesting tristable phenomenon. The analysis for the  $B_{iii}$  is more involved than the  $A_{iii}$  model. We have noticed that the  $C_{iii}$  model was investigated by several authors. For example, Huang *et al.* [2014] gave a quite complete bifurcation analysis on this model including the existence of equilibria and their types, Hopf bifurcation and Bogdanov–Takens bifurcation. Very recently, Dai *et al.* [2019] paid particular attention on Hopf bifurcation on this model and proved the existence of four limit cycles. In another article published very recently, Wang and Zhang [2019] gave a very detailed study for this model under the assumption that the prey reproduces much faster than the predator, i.e.  $s \ll r$  and so that the system becomes a singularly perturbed differential system. The authors then apply the geometric singular perturbation theory (e.g. see [Fenichel, 1979]) to analyze the slow–fast dynamics of the system and showed, in addition to bifurcation of Hopf cycles and relaxation oscillations, richer new dynamical phenomena including canard cycles, canard explosion and relaxation oscillations, heteroclinic and homoclinic orbits.

The paper is organized as follows. In the next section, we present a dynamical analysis on the  $B_{iii}$  model with the main attention on Hopf bifurcation from the positive equilibrium. Then, multiple limit cycles bifurcation is considered in Sec. 3. Simulation results are present in Sec. 4, and finally conclusion is drawn in Sec. 5.

## 2. Stability and Hopf Bifurcation Analysis on the $B_{iii}$ Model

In this section, we consider the dynamics of system  $B_{iii}$ , described by the dimensionless equation (10), and focus on stability and bifurcation, in particular Hopf bifurcation. In order to simplify the analysis, we first use the state scaling and time scaling to reduce system (10) to a dimensionless system with less number of parameters. To achieve this, taking the state scaling:  $x = KX$ ,  $y = \frac{mK}{r}Y$  and time

scaling  $\tau = rt$ , we obtain the following dimensionless system,

System  $B_{iii}$  :

$$\begin{cases} \dot{X} = X \left( 1 - X - \frac{XY}{AX^2 + BXY + Y^2} \right), \\ \dot{Y} = Y \left( \frac{CX^2}{AX^2 + BXY + Y^2} - D \right), \end{cases} \quad (14)$$

where  $A = \frac{r^2}{m^2}a$ ,  $B = \frac{r}{m}b$ ,  $C = \frac{r}{m}c$ ,  $D = \frac{1}{r}d$ .

Note that  $A > 0$ ,  $C > 0$ ,  $D > 0$ , while  $B > -2\sqrt{A}$ , which may take negative values or zero. The system has three equilibrium solutions:

$$\begin{aligned} E_0 : (X_0, Y_0) &= (0, 0); \\ E_1 : (X_1, Y_1) &= (1, 0); \\ E_2 : (X_2, Y_2), \quad \text{where } Y_2 &= \frac{C}{D}X_2(1 - X_2), \\ &(0 < X_2 < 1) \end{aligned} \quad (15)$$

and  $X_2$  is determined from the quadratic equation:

$$\begin{aligned} F_1 &= C^2(1 - X_2)^2 + BCD(1 - X_2) \\ &- D(C - AD) = 0. \end{aligned} \quad (16)$$

Note that the equilibrium  $E_0$  exists because  $X = 0$  and  $Y = 0$  are invariant, and in addition to  $X > 0$ ,  $Y > 0$  we have

$$\begin{aligned} &\lim_{\substack{X \rightarrow 0 \\ Y \rightarrow 0}} \frac{X^2Y}{AX^2 + BXY + Y^2} \\ &= \lim_{\substack{X \rightarrow 0 \\ Y \rightarrow 0}} \frac{Y}{\left(\frac{Y}{X} + \frac{B}{2}\right)^2 + A - \frac{B^2}{4}} \\ &= 0, \quad (B > -2\sqrt{A}). \end{aligned}$$

It is obvious that the biologically meaningful equilibrium solution  $E_2$  satisfies  $X_2 \in (0, 1)$  and so  $Y_2 > 0$ . Solving  $F_1 = 0$  gives two solutions:

$$X_2^\pm = \frac{1}{2C}[2C + BD \pm \sqrt{\Delta}], \quad (17)$$

where

$$\begin{aligned} \Delta &= B^2D^2 + 4D(C - AD) \\ &= (2C + BD)^2 + 4D^2(A^- - A) \\ &= 4D^2(A^* - A), \end{aligned} \quad (18)$$

with

$$A^* = \frac{B^2}{4} + \frac{C}{D}, \quad A^- = \frac{C(D - C - BD)}{D^2}. \quad (19)$$

It is easy to show that  $A^* \geq A^-$  since

$$\begin{aligned} A^* - A^- &= \frac{1}{4D^2}(B^2D^2 + 4C^2 + 4CDB) \\ &= \frac{1}{4D^2}(BD + 2C)^2 \geq 0. \end{aligned}$$

Since the parameters  $A, C, D$  take positive values and  $B > -2\sqrt{A}$ , for the convenience in the following analysis, we transform the condition  $B > -2\sqrt{A}$  as

$$\begin{aligned} \sqrt{A} &> \max\left\{0, -\frac{B}{2}\right\} \quad \text{or} \\ \begin{cases} A > 0 & \text{if } B \geq 0, \\ A > \frac{B^2}{4} & \text{if } B < 0 \end{cases} \end{aligned} \quad (20)$$

and define

$$B^* = -\frac{2}{D}(C + \sqrt{CD}). \quad (21)$$

Then, we have the following results for the existence of  $E_2^\pm$  and coexistence of  $E_2^+$  and  $E_2^-$ . Although the existence of the positive equilibrium  $E_2$  has been discussed in the literature (e.g. see [Lamontagne *et al.*, 2008]), here we want to express the equilibrium more explicitly in terms of the system parameters  $A, B, C$  and  $D$  and so make it easy for the bifurcation analysis.

**Theorem 2.1.** *For the equilibrium  $E_2$  of system  $B_{iii}$  with  $X_2 \in (0, 1)$ , the following results hold.*

- (1) For  $B \in R$  and  $A > A^*$ , there is no equilibrium  $E_2$ .
- (2) For  $B \in (-\frac{2C}{D}, 0)$  and  $A = A^*$ , there exists a unique solution  $E_2^* = (1 + \frac{BD}{2C}, \frac{-B}{2}(1 + \frac{BD}{2C}))$ .
- (3) For  $A < A^*$ ,
  - (3a) if  $B \geq 0$  and  $\max\{0, A^-\} < A < \frac{C}{D}$ , then there exists a unique solution  $E_2^-$ .
  - (3b) If  $B \in (-\frac{2C}{D}, 0)$  and  $\max\{\frac{B^2}{4}, A^-\} < A < A^*$ , then  $E_2^-$  exists; if  $B \in [-\frac{2C}{D}, 0)$  and  $\max\{\frac{B^2}{4}, \frac{C}{D}\} < A < A^*$ , or if  $B \in (B^*, -\frac{2C}{D})$  and  $\max\{\frac{B^2}{4}, \frac{C}{D}\} < A < A^-$ , then  $E_2^+$  exists.

Moreover, for any  $D > 0, C > 0, E_2^-$  and  $E_2^+$  coexist if  $B \in (-\frac{2C}{D}, 0)$  and  $A > \max\{\frac{B^2}{4}, \frac{C}{D}, A^-\}$ .

*Proof*

- (1) The conclusion is obvious since  $\Delta < 0$  when  $A > A^*$ .
- (2) When  $A = A^*$ , we have  $\Delta = 0$  and so

$$X_2^* = X_2^\pm = \frac{1}{2C}(2C + BD) = 1 + \frac{BD}{2C}.$$

Then  $X_2^* < 1$  requires  $B < 0$ , and it follows from  $X_2^* > 0$  that

$$1 + \frac{BD}{2C} < 1 \Leftrightarrow B > -\frac{2C}{D}$$

and so  $-\frac{2C}{D} < B < 0$  is required.

- (3) When  $A < A^*$ ,  $\Delta > 0$ , so both  $X_2^-$  and  $X_2^+$  are real.

- (3a) When  $B \geq 0$ , it is easy to see that

$$\begin{aligned} X_2^+ &= \frac{1}{2C}(2C + BD + \sqrt{\Delta}) \\ &= 1 + \frac{1}{2C}(BD + \sqrt{\Delta}) > 1. \end{aligned}$$

So the equilibrium  $E_2^+$  has no biological meaning, and thus only  $E_2^-$  may exist. In order to have  $X_2^- < 1$ , we need

$$\begin{aligned} 1 + \frac{1}{2C}(BD - \sqrt{\Delta}) < 1 &\Leftrightarrow BD < \sqrt{\Delta} \\ &\Leftrightarrow 0 < 4D(C - AD) \\ &\Leftrightarrow A < \frac{C}{D}. \end{aligned}$$

Next, consider  $X_2^- > 0$  which yields  $1 + \frac{1}{2C}(BD - \sqrt{\Delta}) > 0$ , or  $2C + BD > \sqrt{\Delta}$  from which we have

$$0 > -4D^2(A - A^-) \Leftrightarrow A > A^-$$

and so obtain

$$\max\{0, A^-\} < A < \frac{C}{D}.$$

Note from (19) that  $A^- < \frac{C}{D}$  since  $B \geq 0$ .

- (3b) For  $B < 0, A > \frac{B^2}{4}$ . First we find the conditions under which  $0 < X_2^- < 1$ .  $X_2^- < 1$  is obvious since  $B < 0$ . So we only need to consider  $X_2^- > 0$ , which is equivalent to  $2C + BD > \sqrt{\Delta}$ .

So  $2C + BD > 0$  or  $B > -\frac{2C}{D}$ , yielding  $-\frac{2C}{D} < B < 0$ . Then  $2C + BD > \sqrt{\Delta}$  yields

$$(2C + BD)^2 > (2C + BD)^2 + 4D^2(A^- - A) \\ \Leftrightarrow A > A^-.$$

Hence,  $A > \max\{\frac{B^2}{4}, A^-\}$ .

Next we consider the equilibrium  $E_2^+$ . It is easy to see that  $X_2^+ < 1$  yields

$$BD + \sqrt{\Delta} < 0 \\ \Leftrightarrow \sqrt{\Delta} < -BD \\ \Leftrightarrow B^2D^2 + 4D(C - AD) < B^2D^2 \\ \Leftrightarrow A > \frac{C}{D}.$$

Hence, we have

$$A > \max\left\{\frac{B^2}{4}, \frac{C}{D}\right\}.$$

For  $X_2^+ > 0$ , we have

$$2C + BD + \sqrt{\Delta} > 0.$$

First suppose  $2C + BD \geq 0$  or  $B \geq -\frac{2C}{D}$  which guarantees  $X_2^+ > 0$ . So the first condition given in (3b) for  $0 < X_2^- < 1$  is obtained.

If  $2C + BD < 0$ , we have

$$B < -\frac{2C}{D}$$

and so  $\Delta > (2C + BD)^2$  yields

$$(2C + BD)^2 + 4D^2(A^- - A) > (2C + BD)^2 \\ \Leftrightarrow A < A^-.$$

Combining this with  $A > \max\{\frac{B^2}{4}, \frac{C}{D}\}$  we obtain

$$\max\left\{\frac{B^2}{4}, \frac{C}{D}\right\} < A < A^-,$$

which requires that  $\max\{\frac{B^2}{4}, \frac{C}{D}\} < A^-$ .  $\frac{C}{D} < A^-$  is obvious since  $B < -\frac{2C}{D} < -\frac{C}{D}$ . In order to have  $\frac{B^2}{4} < A^-$ , we need that

$$D^2B^2 + 4CDB + 4C^2 - 4CD < 0 \\ \Leftrightarrow B^* = -\frac{2}{D}(C + \sqrt{CD}) \\ < B < \frac{2}{D}(-C + \sqrt{CD}).$$

Noticing that  $B < -\frac{2C}{D}$  and  $B^* < -\frac{2C}{D} < \frac{2}{D}(-C + \sqrt{CD})$ , we obtain  $B^* < B < -\frac{2C}{D}$ .

The coexistence condition of  $E_2^-$  and  $E_2^+$  is straightforward by comparing the existence conditions given in (3b) for the equilibria  $E_2^-$  and  $E_2^+$ .

The proof of Theorem 2.1 is complete. ■

For the stability of the equilibria  $E_0$  and  $E_1$  we have the following result.

**Theorem 2.2.** For system (14), the dynamics of the equilibrium  $E_0$  is complex.  $E_0$  may be stable or unstable under certain conditions on parameters (with the detailed conditions given in the proof). The equilibrium  $E_1$  is a stable node when  $A > \frac{C}{D}$  and it becomes unstable (a saddle) for  $A < \frac{C}{D}$ . Moreover,  $E_1$  is globally asymptotically stable for  $B \geq 0$  and  $A > \frac{C}{D}$ .  $A = \frac{C}{D}$  defines a critical point at which a bifurcation occurs.

*Proof.* The Jacobian matrix of system (14) is given by

$$J(X, Y) = \begin{bmatrix} 1 - 2X - \frac{(BX + 2Y)XY^2}{(AX^2 + BXY + Y^2)^2} & -\frac{(AX^2 - Y^2)X^2}{(AX^2 + BXY + Y^2)^2} \\ \frac{C(BX + 2Y)XY^2}{(AX^2 + BXY + Y^2)^2} & \frac{C(AX^2 - Y^2)X^2}{(AX^2 + BXY + Y^2)^2} - D \end{bmatrix}. \quad (22)$$

Although the equilibrium  $E_0 : (0, 0)$  is well defined, its stability cannot be simply analyzed by using the Jacobian matrix. In fact, a similar case for the stability of the origin  $(x, y) = (0, 0)$  for system (9) has been studied in [Xiao & Ruan, 2001] in which the authors classify this singular point as a nonhyperbolic critical point (i.e. a critical point of higher

order). The main idea used in [Xiao & Ruan, 2001] is to transform (9) into a polynomial system so that the singular point  $(0, 0)$  is well defined, but then the Jacobian of the new system is a zero matrix making linear analysis not applicable. Based on the new system, it is shown in [Xiao & Ruan, 2001] that any

orbit of the new system tending to the origin must tend to it along a fixed direction. Further, several sectors have been classified in the first quadrant and dynamical properties of the system are explored in each sector. However, as pointed in [Xiao & Ruan, 2001], the information obtained does not provide enough knowledge about the topological structure in the first quadrant around the origin. Therefore, a complete study on such a singular point  $(0, 0)$  is quite challenging.

In this paper, instead of the method used in [Xiao & Ruan, 2001] which analyzes a polynomial

$$\begin{aligned} \dot{r} &= r \left[ \cos^2\theta \left( 1 - r \cos\theta - \frac{\tan\theta}{A + B \tan\theta + \tan^2\theta} \right) + \sin^2\theta \left( \frac{C}{A + B \tan\theta + \tan^2\theta} \right) - D \right], \\ \dot{\theta} &= \sin\theta \cos\theta \left[ \frac{C}{A + B \tan\theta + \tan^2\theta} - D - \left( 1 - r \cos\theta - \frac{\tan\theta}{A + B \tan\theta + \tan^2\theta} \right) \right]. \end{aligned} \tag{23}$$

It is easy to see that  $0$  and  $\frac{\pi}{2}$  are solutions of  $\dot{\theta} = 0$ , for which

$$\begin{aligned} \dot{r}|_{\theta=0} &= r(1 - r) > 0 \quad \text{and} \\ \dot{r}|_{\theta=\frac{\pi}{2}} &= -Dr < 0, \quad \text{as } r \rightarrow 0. \end{aligned}$$

As a matter of fact, one can show that the  $X$ -axis and the  $Y$ -axis are invariant. Therefore, in the following we only consider  $0 < \theta < \frac{\pi}{2}$ . As  $r \rightarrow 0$ ,  $\dot{\theta}$  is reduced to

$$\dot{\theta} = -\frac{\sin\theta \cos\theta F_2}{A + B \tan\theta + \tan^2\theta},$$

system with zero matrix, we directly apply the “blow-up” technique to show a complete set of dynamical structures in the first quadrant around the origin  $E_0$ , indicating that the equilibrium  $E_0$  is unstable. To achieve this, we introduce the blow-up transformation,

$$\begin{aligned} X &= r \cos\theta, \\ Y &= r \sin\theta \end{aligned}$$

and consider the dynamics for  $r \rightarrow 0$ ,  $0 \leq \theta \leq \frac{\pi}{2}$ . Under the above transformation, the system (14) becomes

where  $F_2$  is a quadratic polynomial in  $\tan\theta$  for  $0 < \theta < \frac{\pi}{2}$ :

$$\begin{aligned} F_2(\tan\theta) &= \tan^2\theta + \left( B - \frac{1}{1+D} \right) \tan\theta \\ &\quad + A - \frac{C}{1+D}. \end{aligned} \tag{24}$$

Note that the denominator of  $\dot{\theta}$  is positive since  $B > -2\sqrt{A}$  and  $0 < \theta < \frac{\pi}{2}$ , indicating that  $F_2$  has opposite sign of  $\dot{\theta}$ . The number of roots of the polynomial  $F_2$  for  $\tan\theta$  has three cases: No roots, one root and two roots, according to the following conditions:

$$\begin{aligned} \text{No roots:} & \begin{cases} A \geq \frac{C}{1+D}, \quad B > \frac{1}{1+D}, \quad \text{or} \\ A > \frac{C}{1+D} + \frac{1}{4} \left( B - \frac{1}{1+D} \right)^2, \quad -2\sqrt{A} < B \leq \frac{1}{1+D}; \end{cases} \\ \text{One root:} & \begin{cases} 0 < A < \frac{C}{1+D}, \quad \text{or} \\ A = \frac{C}{1+D}, \quad -2\sqrt{A} < B \leq \frac{1}{1+D}, \quad \text{or} \\ A = \frac{C}{1+D} + \frac{1}{4} \left( B - \frac{1}{1+D} \right)^2, \quad -2\sqrt{A} < B \leq \frac{1}{1+D}; \end{cases} \\ \text{Two roots:} & \frac{C}{1+D} < A < \frac{C}{1+D} + \frac{1}{4} \left( B - \frac{1}{1+D} \right)^2, \quad -2\sqrt{A} < B \leq \frac{1}{1+D}. \end{aligned} \tag{25}$$

Let the one root be  $\tan \theta_1$ , and the two roots be  $\tan \theta_1 > \tan \theta_2$  ( $\theta_1 > \theta_2$ ). Then for the case of no roots,  $F_2 > 0$  and so  $\dot{\theta} < 0$ . Similarly, we can obtain the sign of  $\dot{\theta}$  for the other two cases as follows:

For no roots:  $\dot{\theta} < 0$ ;

$$\text{For one root: } \begin{cases} \dot{\theta} > 0 & \text{for } 0 < \theta < \theta_1, \\ \dot{\theta} < 0 & \text{for } \theta_1 < \theta < \frac{\pi}{2}; \end{cases}$$

$$\text{For two roots: } \begin{cases} \dot{\theta} < 0 & \text{for } 0 < \theta < \theta_2, \\ \dot{\theta} > 0 & \text{for } \theta_2 < \theta < \theta_1, \\ \dot{\theta} < 0 & \text{for } \theta_1 < \theta < \frac{\pi}{2}. \end{cases} \quad (26)$$

Moreover, for the cases of one root and two roots, we need to find the sign of  $\dot{r}$ . As  $r \rightarrow 0$  and  $\dot{\theta} = 0$ , it is easy to use (23) to obtain

$$\begin{aligned} \dot{r} &= r \left( \frac{C}{A + B \tan \theta + \tan^2 \theta} - D \right) \\ &= \frac{r}{A + B \tan \theta + \tan^2 \theta} \\ &\quad \times [C - D(A + B \tan \theta + \tan^2 \theta)] \\ &= \frac{r}{A + B \tan \theta + \tan^2 \theta} (C - D \tan \theta), \end{aligned} \quad (27)$$

implying that  $\dot{r}$  has the same sign of  $C - D \tan \theta$ . Based on the above discussions and formulas, we obtain a total of six topologically different structures near  $E_0$  in the first quadrant, expressed in terms of the system parameters:  $A$ ,  $B$ ,  $C$  and  $D$ . They are classified as follows, with the sign of  $\dot{\theta}$  given in (26).

(i) No roots under one of the following two conditions:

$$(ia) \quad A \geq \frac{C}{1+D}, \quad B > \frac{1}{1+D};$$

$$(ib) \quad B \leq \frac{1}{1+D},$$

$$A > \frac{C}{1+D} + \frac{1}{4} \left( B - \frac{1}{1+D} \right)^2.$$

(ii) One root  $\theta_1 < \tan^{-1}(\frac{C}{D})$  if one of the following three conditions holds:

$$(iia) \quad A < \frac{C}{1+D},$$

$$B > \max \left\{ -2\sqrt{A}, \frac{1}{1+D} - \frac{2C}{D}, 1 - \frac{C}{D} - \frac{AD}{C} \right\};$$

$$(iib) \quad A = \frac{C}{1+D},$$

$$\max \left\{ -2\sqrt{A}, \frac{1}{1+D} - \frac{C}{D} \right\} < B < \frac{1}{1+D};$$

$$(iic) \quad \frac{C}{1+D} < A < \frac{C}{1+D} + \frac{C^2}{D^2},$$

$$B = \frac{1}{1+D} - 2\sqrt{A - \frac{C}{1+D}}.$$

(iii) One root  $\theta_1 > \tan^{-1}(\frac{C}{D})$  if one of the following four conditions is satisfied:

$$(iiia) \quad A < \frac{C}{1+D},$$

$$\max \left\{ -2\sqrt{A}, \frac{1}{1+D} - \frac{2C}{D} \right\} < B < 1 - \frac{C}{D} - \frac{AD}{C};$$

$$(iiib) \quad C \leq \frac{D}{2(1+D)} (1 + D + \sqrt{(1+D)^2 - 1}),$$

$$\max \left\{ 0, \frac{C}{D} - \frac{1}{2(1+D)} \right\} < \sqrt{A} < \sqrt{\frac{C}{1+D}},$$

$$-2\sqrt{A} < B \leq \frac{1}{1+D} - \frac{2C}{D};$$

$$(iiic) \quad C < \frac{D}{1+D} (1 + 2D + \sqrt{(1+2D)^2 - 1}),$$

$$A = \frac{C}{1+D}, \quad -2\sqrt{A} < B \leq \frac{1}{1+D} - \frac{C}{D};$$

$$(iiid) \quad A > \frac{C}{1+D} + \frac{C^2}{D^2},$$

$$B = \frac{1}{1+D} - 2\sqrt{A - \frac{C}{1+D}}.$$

(iv) Two roots  $\theta_2 < \theta_1 < \tan^{-1}(\frac{C}{D})$  under the condition:

$$\frac{C}{1+D} < A < \frac{C}{1+D} + \frac{C^2}{D^2},$$

$$\max\left\{-2\sqrt{A}, 1 - \frac{C}{D} - \frac{AD}{C}\right\}$$

$$< B < \frac{1}{1+D} - 2\sqrt{A - \frac{C}{1+D}}.$$

(v) Two roots  $\theta_2 < \tan^{-1}(\frac{C}{D}) < \theta_1$  under the condition:

$$\max\left\{\sqrt{\frac{C}{1+D}}, \frac{C - \sqrt{CD}}{D}\right\}$$

$$< \sqrt{A} < \sqrt{\frac{C}{1+D} + \frac{C^2}{D^2}},$$

$$\max\left\{-2\sqrt{A}, \frac{1}{1+D} - \frac{2C}{D}\right\}$$

$$< B < 1 - \frac{C}{D} - \frac{AD}{C}.$$

(vi) Two roots  $\tan^{-1}(\frac{C}{D}) < \theta_2 < \theta_1$  under the condition:

$$A > \frac{C}{1+D} + \frac{C^2}{D^2},$$

$$\max\left\{-2\sqrt{A}, 1 - \frac{C}{D} - \frac{AD}{C}\right\}$$

$$< B < \frac{1}{1+D} - 2\sqrt{A - \frac{C}{1+D}}.$$

It should be noted that the condition in (ib) for  $A$  implies  $B > -2\sqrt{A}$ .

The blow-up diagram for Case (i) is shown in Fig. 1(a), from which we can sketch the phase portrait of the original system (14). However, instead of a general sketching diagram, we choose a set of parameter values:  $A = B = C = D = 1$  satisfying the condition (ia) to simulate system (14) to get the phase portrait as depicted in Fig. 1(b), which is more convincing.

We will not prove all the cases listed above, but choose Case (ii) to give a detailed proof and other cases can be similarly proved. Let

$$\Delta_1 = \left(B - \frac{1}{1+D}\right)^2 - 4\left(A - \frac{C}{1+D}\right).$$

There are three possibilities for  $F_2$  to have one root:

- (1)  $0 < A < \frac{C}{1+D}, \quad (\Delta_1 > 0),$
- (2)  $A = \frac{C}{1+D}, \quad -2\sqrt{A} < B < \frac{1}{1+D},$
- (3)  $\Delta_1 = 0, \quad -2\sqrt{A} < B < \frac{1}{1+D},$

which yield the three conditions in (25), under which  $F_2$  has one root  $\theta_1$  such that  $C - D \tan \theta_1 > 0$ . First consider Case (1). Substituting the solution  $\tan \theta_1$  into  $C - D \tan \theta_1$  yields

$$C + \frac{D}{2}\left(B - \frac{1}{1+D}\right)$$

$$> \frac{D}{2}\sqrt{\left(B - \frac{1}{1+D}\right)^2 - 4\left(A - \frac{C}{1+D}\right)}$$

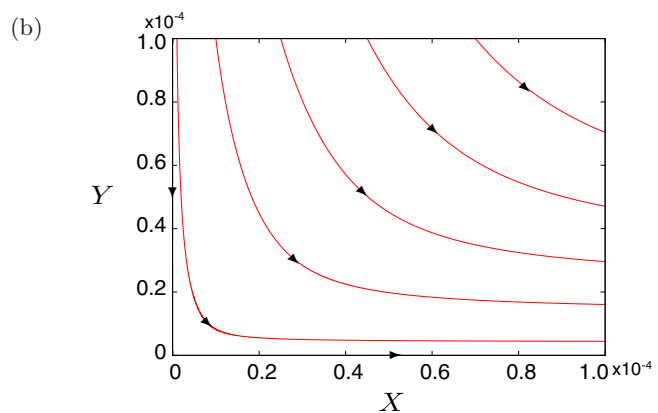
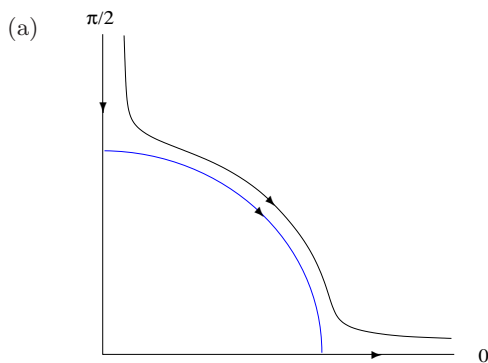


Fig. 1. Dynamics of system (14) in the first quadrant near  $E_0$  for  $\dot{\theta} = 0$  having no roots in  $(0, \frac{\pi}{2})$ : (a) blow-up diagram and (b) simulated phase portrait of the system with  $A = B = C = D = 1$ .

which requires  $C + \frac{D}{2}(B - \frac{1}{1+D}) > 0$ , i.e.  $B > \frac{1}{1+D} - \frac{2C}{D}$ . Then it follows from the above inequality that

$$C^2 + CD\left(B - \frac{1}{1+D}\right) > -AD^2 + \frac{D^2C}{1+D}$$

$$\Leftrightarrow B > 1 - \frac{C}{D} - \frac{AD}{C}$$

and hence the condition (iia) is obtained.

Next, consider Case (ii) for which  $C - D \tan \theta_1 > 0$  becomes

$$C + D\left(B - \frac{1}{1+D}\right) > 0 \Leftrightarrow B > \frac{1}{1+D} - \frac{C}{D},$$

which together with  $-2\sqrt{A} < B < \frac{1}{1+D}$  yields the condition (iib).

For Case (iii), note that  $\Delta_1 = 0$  yields

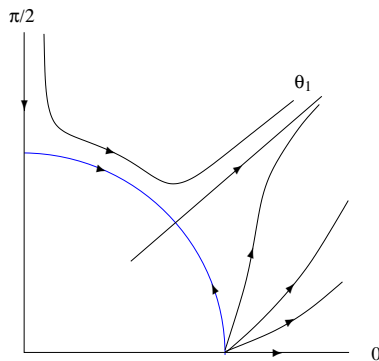
$$A = \frac{C}{1+D} + \frac{1}{4}\left(B - \frac{1}{1+D}\right)^2$$

$$\Rightarrow B = \frac{1}{1+D} - 2\sqrt{A - \frac{C}{1+D}},$$

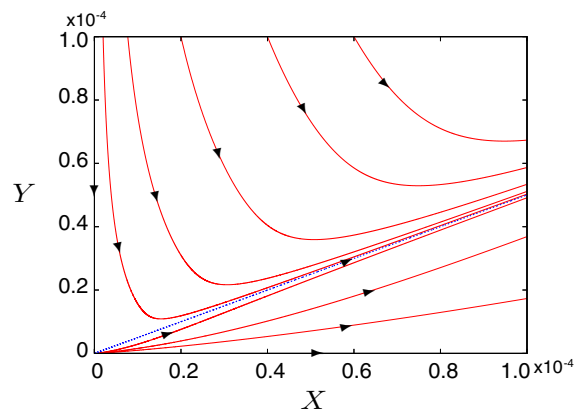
since  $A > \frac{C}{1+D}$  and  $B < \frac{1}{1+D}$ . It is easy to show that  $-2\sqrt{A} < B$  is satisfied because

$$-2\sqrt{A} < \frac{1}{1+D} - 2\sqrt{A - \frac{C}{1+D}}$$

$$\Leftrightarrow \frac{1}{1+D} + 4(C + \sqrt{A}) > 0.$$



(a)



(b)

Fig. 2. Dynamics of system (14) in the first quadrant near  $E_0$  for  $\dot{\theta} = 0$  having one root  $\theta_1 < \tan^{-1}(\frac{C}{D})$ : (a) blow-up diagram and (b) simulated phase portrait of the system with  $A = 0.5$ ,  $B = 0$ ,  $C = D = 1$ , where the blue radial denotes  $\theta = \theta_1 = \tan^{-1} \frac{1}{2}$ .

Now,  $C - D \tan \theta_1 > 0$  is reduced to

$$C + \frac{D}{2}\left(B - \frac{1}{1+D}\right) > 0$$

$$\Leftrightarrow B > \frac{1}{1+D} - \frac{2C}{D}$$

$$\Leftrightarrow \frac{1}{1+D} - 2\sqrt{A - \frac{C}{1+D}} > \frac{1}{1+D} - \frac{2C}{D}$$

$$\Leftrightarrow A < \frac{C}{1+D} + \frac{C^2}{D^2},$$

which gives the condition (iic).

The blow-up diagram for Case (ii) is given in Fig. 2(a), and a simulated phase portrait for the original system (14) with the parameter values:  $A = \frac{1}{2}$ ,  $B = 0$ ,  $C = D = 1$  (belonging to Case (iib)) is shown in Fig. 2(b). It can be seen from this figure that the equilibrium  $E_0$  (i.e. around the origin in the first quadrant) appears to be an unstable node for  $0 < \theta < \theta_1$  while being a saddle for  $\theta_1 < \theta < \frac{\pi}{2}$ , indicating that  $E_0$  is unstable.

The blow-up diagram for Case (iii) with  $C - D \tan \theta_1 < 0$  is shown in Fig. 3(a), and a simulation with the parameter values:  $A = \frac{1}{2}$ ,  $B = -1$ ,  $C = D = 1$  (belonging to Case (iiic)) is given in Fig. 3(b). This figure shows somewhat unusual dynamical behavior, though the  $E_0$  still looks like a saddle for  $0 < \theta < \theta_1$  but now a stable node for  $\theta_1 < \theta < \frac{\pi}{2}$ . Due to the angle direction on the circle (which is blown-up from the origin) not changed, the saddle trajectories in this figure ( $0 < \theta < \theta_1$ ) show an elliptic shape, quite differently from that

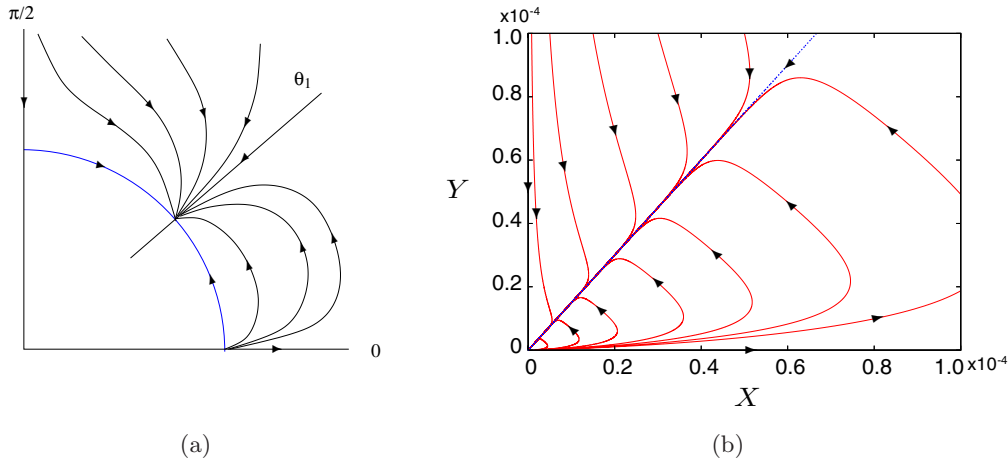


Fig. 3. Dynamics of system (14) in the first quadrant near  $E_0$  for  $\dot{\theta} = 0$  having one root  $\theta_1 > \tan^{-1}(\frac{C}{D})$ : (a) blow-up diagram and (b) simulated phase portrait of the system with  $A = 0.5, B = -1, C = D = 1$ , where the blue radial denotes  $\theta = \theta_1 = \tan^{-1} \frac{3}{2}$ .

shown in Fig. 2(b) ( $\theta_1 < \theta < \frac{\pi}{2}$ ), which is a hyperbolic type.

The blow-up diagrams and phase portraits for the case of two roots (iii) are shown in Figs. 4–6. Note that since  $\theta_1 > \theta_2$  we have  $C - D \tan \theta_1 < C - D \tan \theta_2$  and so there are only three cases when  $F_2$  has two real positive roots.

We have shown in the above discussions that there exist six topologically different phase portraits on the dynamics of the  $B_{iii}$  model near the origin in the first quadrant. It is easy to find the stability of the equilibrium  $E_0$  for Cases (i)–(v), while it is complex for the Case (vi). We summarize the results in Table 1, where DNE denotes “Do Not Exist”, and  $A_1, A_2, B_1$  and  $B_2$  are defined as

$$A_1 = \frac{C}{1+D} + \frac{C^2}{D^2},$$

$$A_2 = \frac{C}{1+D} + \frac{1}{4(1+D)^2},$$

$$B_1 = 1 - \frac{C}{D} - \frac{AD}{C},$$

$$B_2 = \frac{1}{1+D} - 2\sqrt{A - \frac{C}{1+D}}.$$

Now we turn to consider the equilibrium  $E_1 : (1, 0)$ . Evaluating the Jacobian  $J(X, Y)$  in (22) we obtain the eigenvalues as  $-1$  and  $\frac{C}{A} - D$ . Thus, it is a stable node when  $A > \frac{C}{D}$  and becomes unstable

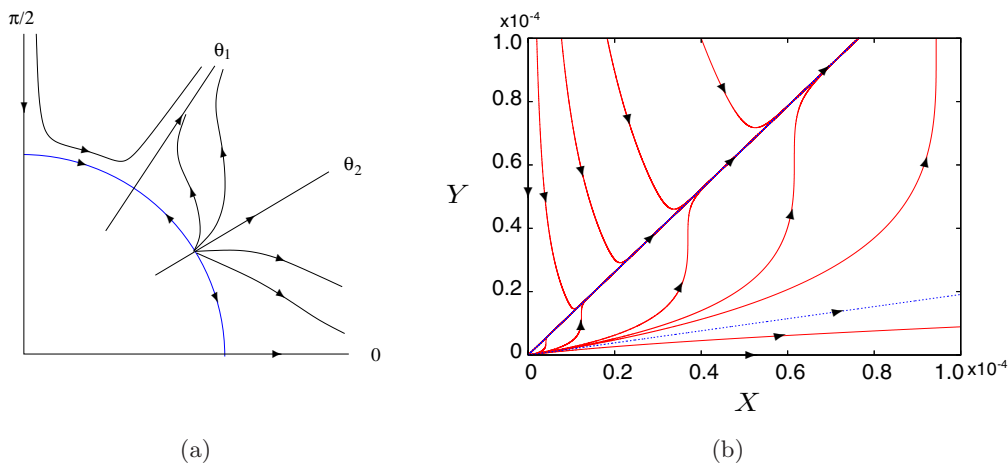


Fig. 4. Dynamics of system (14) in the first quadrant near  $E_0$  for  $\dot{\theta} = 0$  having two roots  $\theta_2 < \theta_1 < \tan^{-1}(\frac{C}{D})$ : (a) blow-up diagram and (b) simulated phase portrait of the system with  $A = 1, B = -1, C = 1.5, D = 1$ , where the two blue radials denote  $\theta = \theta_1 = \tan^{-1}(\frac{3+\sqrt{5}}{4}), \theta_2 = \tan^{-1}(\frac{3-\sqrt{5}}{4})$ .

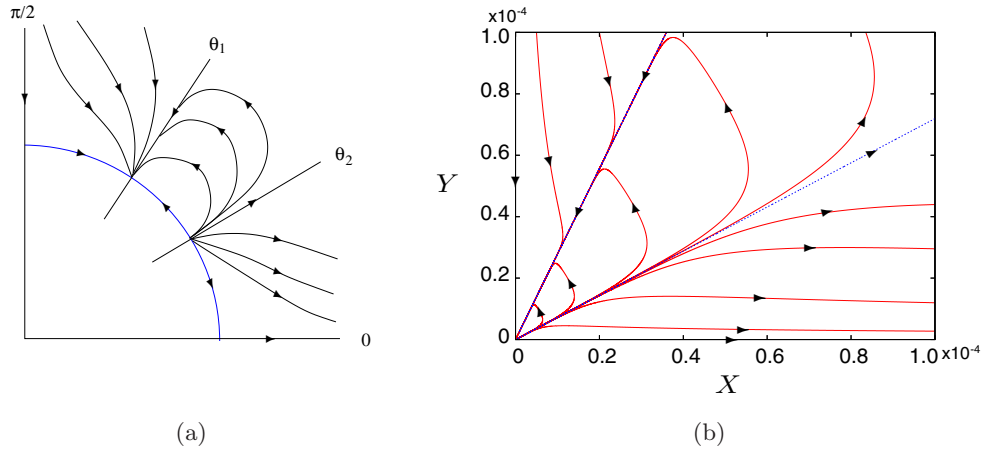


Fig. 5. Dynamics of system (14) in the first quadrant near  $E_0$  for  $\dot{\theta} = 0$  having two roots  $\theta_2 < \tan^{-1}(\frac{C}{D}) < \theta_1$ : (a) blow-up diagram and (b) simulated phase portrait of the system with  $A = 3, B = -3, C = 2, D = 1$ , where the two blue radials denote  $\theta = \theta_1 = \tan^{-1}(\frac{7+\sqrt{17}}{4}), \theta_2 = \tan^{-1}(\frac{7-\sqrt{17}}{4})$ .

(a saddle) for  $A < \frac{C}{D}$ . So  $A = \frac{C}{D}$  defines a critical point at which  $E_1$  loses its stability. This critical point actually defines a transcritical bifurcation between the equilibria  $E_1$  and  $E_2$ , which will be shown in the next theorem.

When  $B \geq 0$ , we can show that  $E_1$  is globally asymptotically stable for  $A > \frac{C}{D}$ . In fact, for  $A > \frac{C}{D}$ , i.e.  $C < AD$ , there exists a trapping region with no interior equilibria, but a saddle  $E_0$ , and a stable node  $E_1$ , both of them are located on the boundary of the trapping region  $R$ , indicating that all trajectories converge to  $E_1$ . We may construct a Lyapunov function to analytically prove this. Let

$$V_1 = \frac{1}{2}(X - 1)^2 + \frac{1}{AD - C}Y.$$

Then, we have

$$\begin{aligned} \left. \frac{dV_1}{d\tau} \right|_{(14)} &= (X - 1)\dot{X} + \frac{1}{AD - C}\dot{Y} \\ &= (X - 1)X \left( 1 - X - \frac{XY}{AX^2 + BXY + Y^2} \right) \\ &\quad + \frac{Y}{AD - C} \left( \frac{CX^2}{AX^2 + BXY + Y^2} - D \right) \\ &= -X(X - 1)^2 \\ &\quad - \frac{Y[(AD - C)X^3 + DY(BX + Y)]}{(AD - C)(AX^2 + BXY + Y^2)} \\ &\leq 0, \quad \text{for } A > \frac{C}{D} \end{aligned}$$

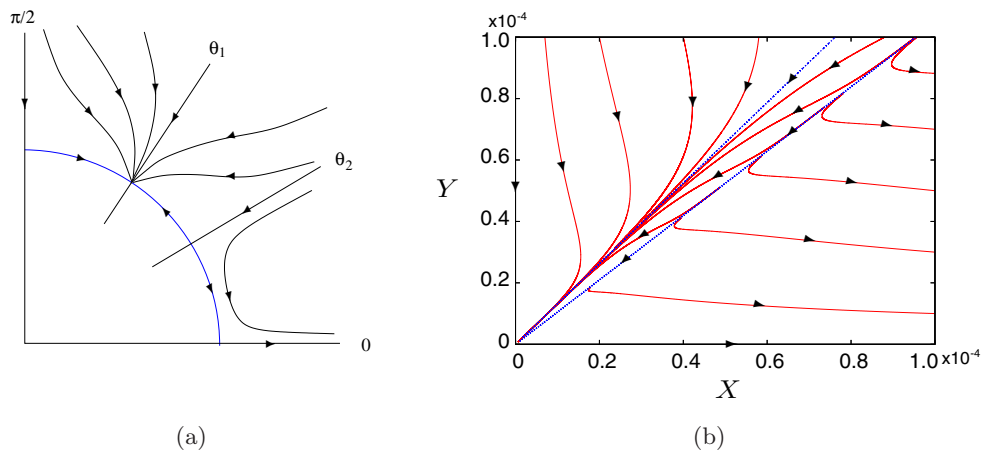


Fig. 6. Dynamics of system (14) in the first quadrant near  $E_0$  for  $\dot{\theta} = 0$  having two roots  $\tan^{-1}(\frac{C}{D}) < \theta_2 < \theta_1$ : (a) blow-up diagram and (b) simulated phase portrait of the system with  $A = 1.875, B = -1.86, C = D = 1$ , where the two blue radials denote  $\theta = \theta_1 = \tan^{-1} 1.3119, \theta_2 = \tan^{-1} 1.0481$ .

Table 1. Stability of  $E_0$  for system (14).

Case	Additional Conditions	$E_1$	$E_2^\pm$	$E_0$
(i)				Unstable
(ii)				Unstable
(iii)				Stable
(iv)				Unstable
(v)	$\max\left\{\sqrt{\frac{C}{1+D}}, \frac{C-\sqrt{CD}}{D}\right\} < \sqrt{A} < \sqrt{\frac{C}{D}}$	Saddle	DNE	Stable
	$\frac{C}{D} < A < \frac{C}{1+D} + \frac{C^2}{D^2}$	Stable node		Unstable
(vi)	$A > \max\left\{\frac{C}{D}, \frac{C}{1+D} + \frac{C^2}{D^2}\right\}$	Stable node		Unstable
	$\max\{-2\sqrt{A}, B_1\} < B < B_2$			
	$B_1 < B < B_2$ , and			
	(a) $C < \frac{D}{1+D}$ , $A_1 < A < \max\left\{A^-, \frac{B^2}{4}\right\}$			
	or	Saddle	DNE	Stable
	(b) $\begin{cases} \frac{D}{4(1+D)} < C < \frac{D}{1+D}, \\ \max\{A^-, A_2\} < A < \frac{C}{D} \end{cases}$			
	Otherwise	Saddle	$E_2^-$ exists	Unknown

and  $\frac{dV_1}{dt}|_{(14)} = 0$  if and only if  $(X, Y) = (0, 0)$  or  $(X, Y) = (1, 0)$ . But the origin (i.e. the  $E_0$ ) is unstable, hence  $E_1$  is attractive, together with the local stability, implying that  $E_1$  is globally asymptotically stable. ■

For the stability of the equilibria  $E_2^*$ ,  $E_2^-$  and  $E_2^+$ , we have the following theorem.

**Theorem 2.3.** *For system (14), the equilibrium  $E_2^* = (1 + \frac{BD}{2C}, \frac{-B}{2}(1 + \frac{BD}{2C}))$  is a degenerate node for  $B \in (-\frac{2C}{D}, 0)$  when  $A = \frac{B^2}{4} + \frac{C}{D}$ . There is a transcritical bifurcation between  $E_1$  and  $E_2$ . Moreover, the equilibrium  $E_2^+$  is a saddle, while the equilibrium  $E_2^-$  is asymptotically stable (unstable) if the trace of the Jacobian evaluated at  $E_2^-$  is negative (positive).*

*Proof.* Following the classification given in Theorem 2.1 for the existence of  $E_2$ , we first consider the stability of  $E_2^*$  in class (2). Using the Jacobian (22) evaluated at  $E_2^*$  we obtain two eigenvalues:  $-(1 + \frac{BD}{C})$  and 0, and their corresponding vectors are  $(1, 0)$  (along the  $X$ -axis) and  $(D, -(BD + C))$ , respectively. More precisely, we apply center manifold theory to determine the direction of the trajectory moving along the eigenvector  $(D, -(BD + C))$ . To achieve this, we first introduce the following affine transformation:

$$\begin{aligned} X &= X_2 - Dx_1 + x_2, \\ Y &= Y_2 + (C + BD)x_1, \end{aligned} \tag{28}$$

into (14) to obtain

$$\begin{aligned} \dot{x}_1 &= -\frac{BD^2(BD + 2C)}{4(BD + C)}x_1^2 + \frac{B^2D^2}{2(BD + C)}x_1x_2 - \frac{B^3D^2(BD + 2C)}{4(BD + C)(BD + 2C)}x_2^2 + O(|(x_1, x_2)|^3), \\ \dot{x}_2 &= -\frac{BD + C}{C}x_2 - \frac{D^2[B^2(B - C)D^2 + BC(3B - 2C + 4)D + 2(B + 2)C^2]}{4C(BD + C)}x_1^2 \end{aligned}$$

$$\begin{aligned}
 & + \frac{D[B^2(B - C)D^2 + BC(B - 4)D - 4C^2]}{2C(BD + C)}x_1x_2 \\
 & - \frac{B^3(B - C)D^3 + B^2C(B + 4)D^2 + 12BC^2D + 8C^3}{4C(BD + C)(BD + 2C)}x_2^2 + O(|(x_1, x_2)|^3).
 \end{aligned} \tag{29}$$

In the following, we consider the above system (29) up to only second-order terms. Applying center manifold theory and letting

$$\begin{aligned}
 x_2 &= -\frac{D^2M}{4(BD + C)^2}x_1^2, \quad \text{where} \\
 M &= B^2(B - C)D^2 + BC(3B - 2C + 4)D \\
 &+ 2(B + 2)C^2, \tag{30}
 \end{aligned}$$

yields the differential equation on the center manifold as

$$\dot{x}_1 = -\frac{BD^2(BD + 2C)}{4(BD + C)}x_1^2. \tag{31}$$

Returning to the original variable, we use (28), (30) and (31) to obtain

$$\dot{Y} = -\frac{BD^2(BD + 2C)}{4(BD + C)^3}(Y - Y_2)^2, \tag{32}$$

which indicates that  $Y$  is decreasing (increasing) when a trajectory goes through  $E_2^*$  if  $BD + C < 0$  ( $> 0$ ). The phase portraits near  $E_2^*$  are shown in Fig. 7.

In the following we consider the equilibrium  $E_2$  classified in Cases (iiia) and (iiib).

Since  $E_2^+$  only exists in Case (iiib), we next prove that  $E_2^+$  is always a saddle. To achieve this, a direct but tedious evaluation on the Jacobian  $J$

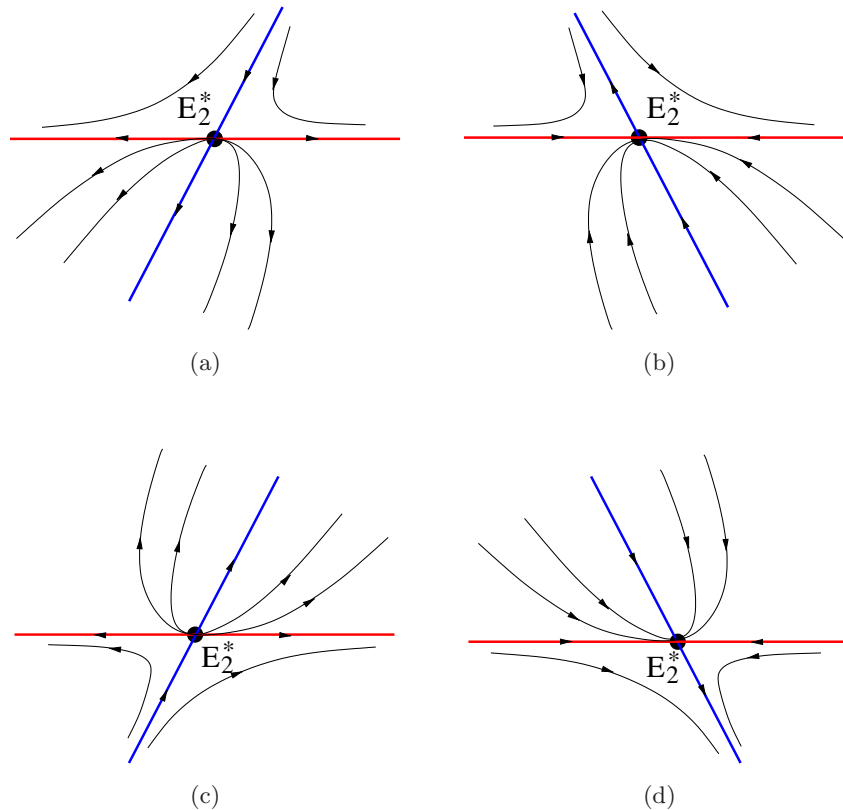


Fig. 7. Phase portraits of the  $B_{iii}$  model near the equilibrium  $E_2^*$ : (a) for  $B \in (-\frac{2C}{D}, -\frac{C}{D})$ ,  $M > 0$ , (b) for  $B \in (-\frac{C}{D}, 0)$ ,  $M > 0$ , (c) for  $B \in (-\frac{2C}{D}, -\frac{C}{D})$ ,  $M < 0$  and (d) for  $B \in (-\frac{C}{D}, 0)$ ,  $M < 0$ .

(22) at  $E_2^+ : (X_2^+, Y_2^+)$  yields

$$\begin{aligned} \det(J_2^+) &= \frac{1}{2C^2} \{ (C + BD)\Delta + D[B(C + BD) \\ &\quad + 2(C - AD)]\sqrt{\Delta} \} \\ &= \frac{\sqrt{\Delta}}{2C^2} \{ 2D(C - AD) \\ &\quad + (C + BD)(\sqrt{\Delta} + BD) \} \\ &= \frac{\sqrt{\Delta}}{2C^2} \left\{ 2D(C - AD) \right. \\ &\quad \left. + (C + BD) \frac{4D(C - AD)}{\sqrt{\Delta} - BD} \right\} \\ &= \frac{D(C - AD)\sqrt{\Delta}}{C^2} \left\{ 1 + \frac{2(C + BD)}{\sqrt{\Delta} - BD} \right\} \\ &= \frac{D(C - AD)\sqrt{\Delta}}{C^2(\sqrt{\Delta} - BD)} (\sqrt{\Delta} + 2C + BD). \end{aligned} \tag{33}$$

Since both conditions given in (iiib) for  $X_2^+$  have  $B < 0$  and  $C < AD$ , we have

$$\frac{D(C - AD)\sqrt{\Delta}}{C^2(\sqrt{\Delta} - BD)} < 0.$$

Thus,  $\det(J_2^+) < 0$  is equivalent to the factor,  $\sqrt{\Delta} + 2C + BD$ , being positive. For the first condition,  $-\frac{2C}{D} \leq B < 0$  yields  $2C + BD > 0$ , and so the factor is positive. For the second condition, since  $B < -\frac{2C}{D}$  (i.e.  $2C + BD < 0$ ) and  $A < A^-$ , we can also prove that  $\sqrt{\Delta} + 2C + BD > 0$  as follows:

$$\begin{aligned} \sqrt{\Delta} &> -(2C + BD) \\ &\Leftrightarrow (2C + BD)^2 + 4D^2(A^- - A) \\ &\quad > (2C + BD)^2 \\ &\Leftrightarrow A < A^-. \end{aligned}$$

This shows that the equilibrium  $E_2^+$  is always unstable (a saddle) when it exists. Therefore, to study stability and bifurcation of  $E_2$  we only need to focus on the equilibrium  $E_2^-$ . Now we show that the determinant of the Jacobian (22) evaluated at  $E_2^-$  is always positive, and thus the stability of  $E_2^-$  is determined by the trace of the Jacobian. Similarly evaluating the Jacobian (22) at  $E_2^-$  we obtain

$$\begin{aligned} \det(J_2^-) &= \frac{1}{2C^2} \{ (C + BD)\Delta \\ &\quad - D[B(C + BD) + 2(C - AD)]\sqrt{\Delta} \} \\ &= \frac{\sqrt{\Delta}}{2C^2} \{ (C + BD)(\sqrt{\Delta} - BD) \\ &\quad - 2D(C - AD) \} \\ &= \frac{\sqrt{\Delta}}{2C^2} \left\{ (C + BD) \frac{4D(C - AD)}{\sqrt{\Delta} + BD} \right. \\ &\quad \left. - 2D(C - AD) \right\} \\ &= \frac{D\sqrt{\Delta}}{C^2} \times \frac{C - AD}{\sqrt{\Delta} + BD} \times (2C + BD - \sqrt{\Delta}) \\ &= \frac{D^2\sqrt{\Delta}}{C^2} \times \frac{\sqrt{\Delta} - BD}{2C + BD + \sqrt{\Delta}} \times (A - A^-). \end{aligned} \tag{34}$$

We shall use the last second equation in (34) to prove the Case (iiia) and the last equation in (34) to prove the Case (iiib). For the condition given in (iiia):  $B \geq 0$ ,  $\max\{0, A^-\} < A < \frac{C}{D}$ , we have  $C > AD$ , and

$$\begin{aligned} 2C + BD - \sqrt{\Delta} &> 0 \Leftrightarrow 0 > 4D^2(A^- - A) \\ &\Leftrightarrow A > A^-. \end{aligned}$$

For the condition given in (iiib):  $-\frac{2C}{D} < B < 0$ ,  $A > \max\{\frac{B^2}{4}, A^-\}$ , we have  $2C + BD > 0$  and  $A > A^-$ , and so  $\det(J_2^-) > 0$ .

It is seen from (16) that  $X_2 = 1$  at  $C = AD$ , which is actually a transcritical bifurcation point between  $E_1$  and  $E_2$ , shown as follows. Note that at  $(X_2, C) = (1, AD)$ ,  $\det(J_2^-) = 0$  and it is easy to show that at this point,  $\text{Tr}(J_2^-) = -1$ . This implies that the critical point at which  $E_1$  loses stability is also a critical point for  $E_2$  to become stable, i.e. this critical point is indeed a transcritical bifurcation point between  $E_1$  and  $E_2$ . Therefore, the only possible bifurcation arising from  $E_2^-$  is Hopf bifurcation.

Summarizing the above results shows that the stability of the equilibrium  $E_2^-$  is fully determined by the trace of the Jacobian (22) evaluated at  $E_2^-$ . Let the trace be  $\text{Tr}(J_2^-)$ . Then, the equilibrium  $E_2^-$  is asymptotically stable (unstable) if  $\text{Tr}(J_2^-) > 0$  ( $< 0$ ). At the critical point determined by  $\text{Tr}(J_2^-) = 0$ , Hopf bifurcation occurs from  $E_2^-$ . ■

More precisely, for the stability of the equilibrium  $E_2^-$  and the Hopf bifurcation occurring from  $E_2^-$ , we have the following theorem.

**Theorem 2.4.** *Let*

$$B = \frac{D(C - AD) - C^2(1 - X_2)^2}{CD(1 - X_2)} \quad (35)$$

and define

$$A_H = \frac{C^2}{D^2}(1 - X_2)^2 + \frac{C(D + X_2)}{D(1 + D - X_2)}, \quad (36)$$

then for any  $D > 0$  and  $0 < X_2 < \frac{1}{2}$ , Hopf bifurcation occurs from  $E_2^-$  at the critical point  $A = A_H$  when  $C$  takes values from the following intervals:

$$C \in \left(0, \frac{D(1 - 2X_2)}{2(1 - X_2)^2(1 + D - X_2)}\right), \quad \text{for } B \geq 0,$$

$$C \in \left(\frac{D(1 - 2X_2)}{2(1 - X_2)^2(1 + D - X_2)}, \infty\right),$$

for  $-2\sqrt{A} < B < 0$ .

(37)

Otherwise, Hopf bifurcation does not exist and the equilibrium  $E_2^-$  is asymptotically stable. When a Hopf bifurcation occurs, the existing equilibrium  $E_2^-$  is asymptotically stable for  $0 < A < A_H$  and unstable for  $A > A_H$ .

*Proof.* Since the explicit solution  $X_2$  solved from the quadratic polynomial equation  $F_1 = 0$  causes much difficulty in the analysis of stability and bifurcation, we solve  $B$  from the equation  $F_1 = 0$  to obtain the expression for  $B$  given in (35) for  $0 < X_2 < 1$ . Then, evaluating the Jacobian of (22) at  $E_2^-$  yields its determinant and trace as

$$\det(J_2^-) = \frac{X_2}{C}[D(C - AD) + C^2(1 - X_2)^2],$$

$$\text{Tr}(J_2^-) = \frac{-1}{CD}\{(1 + D - X_2)[C^2(1 - X_2)^2 - AD^2] + DC(D + X_2)\}.$$
(38)

Hopf bifurcation occurs at the critical point determined by  $\text{Tr}(J_2^-) = 0$ ,  $\det(J_2^-) > 0$ . It follows from

$$\det(J_2^-)|_{\text{Tr}(J_2^-)=0} = \frac{DX_2(1 - 2X_2)}{1 + D - X_2}$$

that Hopf bifurcation can occur from  $E_2^-$  only if

$$0 < X_2 < \frac{1}{2}. \quad (39)$$

This implies that if the equilibrium  $E_2^-$  appears for  $\frac{1}{2} \leq X_2 < 1$ , then it must be asymptotically stable.

In the following, we study the Hopf bifurcation from the equilibrium  $E_2^-$ , and will derive the conditions under which Hopf bifurcation occurs. We consider the cases (3a) and (3b) separately.

**(3a).** When  $B \geq 0$  and  $\max\{0, A^-\} < A < \frac{C}{D}$ ,  $E_2^-$  exists. Now due to (35), we can show that  $A^- < A$  for any value of  $A$ :

$$A^- = \frac{C}{D^2}(D - C - BD)$$

$$= \frac{C}{D^2}\left[D - C - D\frac{D(C - AD) - C^2(1 - X_2)^2}{CD(1 - X_2)}\right]$$

$$= \frac{C^2X_2^2 - C(C + D)X_2 + AD^2}{D^2(1 - X_2)}$$

$$= A - \frac{X_2}{D^2(1 - X_2)}[(1 - X_2)C^2 + D(C - AD)]$$

$< A$ ,

since  $C > AD$  and  $0 < X_2 < 1$ . Note that  $A^-$  may be negative. Thus we can ignore  $A^-$  and have  $0 < A < \frac{C}{D}$ . To find the condition for Hopf bifurcation, we solve  $A$  from  $\text{Tr}(J_2^-) = 0$  to obtain the critical point  $A_H$  given in (36) and then  $B$  given in (35) becomes

$$B_H = -\frac{2C}{D}(1 - X_2) + \frac{1 - 2X_2}{(1 - X_2)(1 + D - X_2)}. \quad (40)$$

It is obvious that  $A_H > 0$  for  $X_2 \in (0, \frac{1}{2})$ . Then taking  $A = A_H$  and using the conditions  $C > AD$  and  $B \geq 0$  we obtain

$$C - A_H D = C\left[\frac{1 - 2X_2}{1 + D - X_2} - \frac{C}{D}(1 - X_2)^2\right]$$

$> 0$  and

$$B_H \geq 0,$$

which result in the condition for  $C$  defined in (37) for the case  $B \geq 0$ .

**(3b).** When  $B \in (-\frac{2C}{D}, 0)$  and  $\max\{\frac{B^2}{4}, A^-\} < A < A^*$ ,  $E_2^-$  exists. We can still use  $B$  given in (35)

and  $A_H$  given in (36) for this case. We can also show that  $0 < X_2 < \frac{1}{2}$ . Therefore, we have

$$\frac{B^2}{4} < A < A^* = \frac{B^2}{4} + \frac{C}{D}.$$

Then, taking  $A = A_H$  and using  $B = B_H$  given in (36) and (40) as well as  $-\frac{2C}{D} < B < 0$  and  $\frac{B^2}{4} < A < A^*$  we get

$$-\frac{2C}{D} < B_H < 0, \quad A_H > \frac{B_H^2}{4} \quad \text{and}$$

$$\frac{B_H^2}{4} + \frac{C}{D} > A_H.$$

Thus, for  $D > 0, C > 0, X_2 \in (0, \frac{1}{2})$ , it is obvious that

$$B_H + \frac{2C}{D} = \frac{2CX_2}{D} + \frac{1 - 2X_2}{(1 - X_2)(1 + D - X_2)} > 0.$$

Also note that

$$\frac{B_H^2}{4} + \frac{C}{D} - A_H = \frac{(1 - 2X_2)^2}{4(1 - X_2)^2(1 + D - X_2)^2} > 0.$$

So we only need to consider  $B_H < 0$  and  $A_H > \frac{B_H^2}{4}$ . A direct computation shows that  $B_H < 0$  gives

$$C > C_1 = \frac{D(1 - 2X_2)}{2(1 - X_2)^2(1 + D - X_2)}$$

and  $A_H > \frac{B_H^2}{4}$  yields

$$C > C_2 = \frac{D(1 - 2X_2)^2}{4(1 - X_2)^2(1 + D - X_2)^2}.$$

Since  $C_1 > C_2 > 0$ , the required condition on  $C$  is  $C > C_1$ , as given in (37) for the case  $-2\sqrt{A} < B < 0$ .

Finally, the transversality condition for the Hopf bifurcation is given by

$$\begin{aligned} H_{\text{transversality}} &= \frac{1}{2} \frac{\partial \text{Tr}(J_2^-)}{\partial A} \Big|_{A=A_H} \\ &= \frac{D}{2C} (1 + D - X_2) > 0, \end{aligned}$$

which does indicate that the Hopf bifurcation occurs at the critical point  $A = A_H$ .

The proof is complete. ■

### 3. Multiple Limit Cycles Bifurcation

Having obtained the explicit conditions for the model  $B_{\text{iii}}$  to have Hopf bifurcation in the last

section, we now consider multiple limit cycles bifurcation in model  $B_{\text{iii}}$ . It has been shown in Theorem 2.4 that Hopf bifurcation occurs for both cases  $B \geq 0$  and  $B < 0$ . However, one question remains: what is the maximal number of limit cycles which can bifurcate from a Hopf critical point? In other words, what is the codimension of the Hopf bifurcation?

We first present some preliminary result which on limit cycle theory, can be used in the next subsection. Suppose a nonlinear dynamical system is described in the form  $\dot{x} = f(x, \mu)$ , where  $\mu$  represents a parameter vector, which has a Hopf bifurcation from the origin, i.e.  $f(0, 0) = 0$  and  $Df(0, 0)$  contains a pair of purely imaginary eigenvalues. Then, we may apply normal form theory (e.g. see [Chow *et al.*, 1994; Gazor & Yu, 2012; Guckenheimer & Holmes, 1993; Kuznetsov, 1998]), as well as the computational methods using computer algebra systems (e.g. see [Han & Yu, 2012; Tian & Yu, 2013, 2014; Yu, 1998; Yu & Leung, 2003]) to obtain the normal form expressed in polar coordinates:

$$\begin{aligned} \dot{r} &= r(v_0 + v_1 r^2 + v_2 r^4 + \dots + v_k r^{2k} + \dots), \\ \dot{\theta} &= \omega_c + \tau_0 + \tau_1 r^2 + \tau_2 r^4 + \dots + \tau_k r^{2k} + \dots, \end{aligned} \tag{41}$$

where  $r$  and  $\theta$  represent the amplitude and phase of motion, respectively.  $v_k$  ( $k = 0, 1, 2, \dots$ ) is called the  $k$ th-order focus value.  $v_0$  and  $\tau_0$  are obtained from linear analysis. The first equation of (41) can be used for studying bifurcation and stability of multiple limit cycles, while the second equation can be used to determine the frequency of the bifurcating periodic motion. Moreover, the coefficients  $\tau_j$  can be used to determine the order or critical periods of a center (i.e. when  $v_j = 0, j \geq 0$ ). The Maple programs developed in [Tian & Yu, 2013, 2014; Yu, 1998] for computing the normal form of Hopf bifurcation have been cross-verified for many mathematical and practical systems. The normal forms obtained by using the different programs are either identical or different by only a positive constant multiplier.

Having obtained these focus values (or the Lyapunov constants) for a given dynamical system, one may use them to determine bifurcation of limit cycles. First, find the critical conditions such that  $v_0 = v_1 = \dots = v_{k-1} = 0$ , but  $v_k \neq 0$ , and then perform appropriate small perturbations to prove the existence of  $k$  limit cycles. The following lemma gives sufficient conditions for the existence

of  $k$  small-amplitude limit cycles. (The proof can be found in [Yu & Han, 2005].)

**Lemma 3.1.** *Suppose a dynamical system, given by  $\dot{x} = f(x, \mu)$ , where  $x \in \mathbb{R}^n$ ,  $\mu = (\mu_1, \mu_2, \dots, \mu_k) \in \mathbb{R}^k$ , has a Hopf bifurcation from the origin at the critical point  $\mu = \mu_c$ , and the corresponding focus values are expressed as*

$$v_j = v_j(\mu), \quad j = 0, 1, \dots, k, \quad (42)$$

satisfying

$$\begin{aligned} v_j(\mu_c) &= 0, \quad j = 0, 1, \dots, k-1, \\ v_k(\mu_c) &\neq 0 \quad \text{and} \\ \det \left[ \frac{\partial(v_0, v_1, \dots, v_{k-1})}{\partial(\mu_1, \mu_2, \dots, \mu_k)}(\mu_c) \right] &\neq 0. \end{aligned} \quad (43)$$

Then, the dynamical system can have  $k$  limit cycles around the origin for some values of  $\mu$  near the critical point  $\mu_c$ .

The result on the multiple limit cycle bifurcation in the  $B_{iii}$  model is given in the following theorem.

**Theorem 3.1.** *The  $B_{iii}$  model can have Hopf bifurcation for both cases  $B \geq 0$  and  $-2\sqrt{A} < B < 0$ . Moreover, the codimension of the Hopf bifurcation is one for  $B \geq 0$  and two for  $-2\sqrt{A} < B < 0$ .*

*Proof.* First, consider the Case (iiia)  $B \geq 0$ . In order to determine stability of the limit cycles bifurcating from the equilibrium  $E_2^-$ , we need to compute focus values. For simplicity, we solve the equilibrium equation and the trace of the Jacobian for the parameters  $A$  and  $B$  to obtain the solution  $A = A_H$  and  $B$  given in (35) and multiply equation (14) by  $AX^2 + BXY + Y^2$ , yielding

$$\omega_c = CX_2^2 \sqrt{\frac{X_2(1-2X_2)}{D(1+D-X_2)}} > 0, \quad \forall X_2 \in \left(0, \frac{1}{2}\right).$$

Then, executing our Maple program [Yu, 1998] we obtain the following focus values:

$$\begin{aligned} v_1 &= \frac{CX_2}{8D^3(D+X_2)(1-2X_2)(1-X_2)(1+D-X_2)} \{2(1+D-X_2)^2[D(1-2X_2) \\ &\quad - C(1-X_2)^2(1+D-X_2)]^2 + (4DX_2 - D - 2 + 10X_2 - 10X_2^2)D(1+D-X_2) \\ &\quad \times [D(1-2X_2) - C(1-X_2)^2(1+D-X_2)] - D^2(1-2X_2) \\ &\quad \times [D + D^2 + 2X_2^3 + X_2(1-2X_2)(4+4D-X_2)]\}, \\ v_2 &= -\frac{C}{192D^6 X_2(D+X_2)^4(1+D-X_2)^2(1-X_2)^3(1-2X_2)^3} \{\dots\}, \end{aligned}$$

where the lengthy expression of  $v_2$  is omitted.

The existence of one limit cycle is obvious, as long as the parameter values are chosen from that defined in Theorem 2.4 such that  $v_1 \neq 0$ , and the limit cycle is stable (unstable) if  $v_1 < 0$  ( $v_1 > 0$ ). To have two limit cycles, it requires  $v_1 = 0$  (but  $v_2 \neq 0$ ). It follows from the conditions given in (35) that  $0 < C \leq \frac{D(1-2X_2)}{2(1-X_2)^2(1+D-X_2)}$ . Let

$$\begin{aligned} C &= C^* - \tilde{C}, \quad \text{where} \\ C^* &= \frac{D(1-2X_2)}{2(1-X_2)^2(1+D-X_2)}, \\ &\quad (C^*, \tilde{C} > 0). \end{aligned} \quad (44)$$

Then, for  $0 < C \leq C^*$ , we have  $\tilde{C} \in (0, C^*]$ . Consequently, the factor in the script bracket of  $v_1$

becomes  $A_2\tilde{C}^2 + A_1\tilde{C} + A_0 \equiv F_3(\tilde{C})$ , where

$$\begin{aligned} A_2 &= 2(1-X_2)^4(1+D-X_2)^4 > 0, \\ A_1 &= D(1-X_2)^2(1+D-X_2)^2 \\ &\quad \times [D + 2X_2(2-3X_2)] > 0, \\ A_0 &= -\frac{1}{2}D^2(1+2D)(1-2X_2) \\ &\quad \times [1-3X_2^2 + D(1-X_2)] < 0, \end{aligned} \quad (45)$$

where  $0 < X_2 < \frac{1}{2}$ , which implies that the quadratic polynomial equation  $F_3(\tilde{C}) = 0$  has two real solutions:  $\tilde{C}^\pm = \frac{1}{2A_2}(-A_1 \pm \sqrt{A_1^2 - 4A_2A_0})$ , satisfying  $\tilde{C}^- < 0 < \tilde{C}^+$ . However, it can be shown that  $\tilde{C}^+ > C^*$ , outside the feasible range of  $\tilde{C}$ . Therefore,

there are no feasible solutions which satisfy  $v_1 = 0$ , and thus two limit cycles are not possible. Moreover, it follows from  $F_3(0) = A_0 < 0$  and  $\tilde{C}^+ > C^*$  that the quadratic polynomial  $F_3 < 0$ , i.e.  $v_1 < 0$ , for  $\tilde{C} \in (0, C^*)$ , implying that the codimension of the Hopf bifurcation is one and the bifurcation is supercritical, yielding stable limit cycles. It should be noted that there are infinitely many feasible solutions for the bifurcation of one small-amplitude limit cycle as long as one chooses  $X_2 \in (0, \frac{1}{2})$  and  $\tilde{C} \in (0, C^*)$ . For example, we take  $D = 1$ ,  $X_2 = \frac{1}{4}$ , and  $\tilde{C} = \frac{31}{126} \in (0, \frac{16}{63})$ , and then use (35) and (44) to obtain  $C = \frac{1}{126}$ ,  $A = \frac{23}{4032}$  and  $B = \frac{31}{84}$ . Hence, for Case (i):  $B \geq 0$ , the  $B_{iii}$  model can have only one small-amplitude limit cycle which can bifurcate from  $E_2^-$  due to Hopf bifurcation. There exists an infinite number of solutions on the parameters and one solution is given below:

$$A = \frac{23}{4032}, \quad B = \frac{31}{84}, \quad C = \frac{1}{126}, \quad D = 1, \tag{46}$$

under which  $v_0 = 0$  and  $v_1 = -\frac{5413}{144506880} < 0$ , indeed indicating that the limit cycle is stable.

Next, consider the Case (iiib)  $-2\sqrt{A} < B < 0$ . We apply the focus values to study limit cycles bifurcating from  $E_2^-$  due to Hopf bifurcation. Note that for this case, we can still apply the same formulas used for Case (iiia) but allow  $B$  to take negative values in the interval  $B \in (-2\sqrt{A}, 0)$ . Thus, it is now assumed that  $B < 0$  in both Eqs. (35) and (44). To have two limit cycles, we may take the negative root of the quadratic polynomial  $F_3(\tilde{C})$ ,  $\tilde{C}^- = \frac{1}{2A_2}(-A_1 - \sqrt{A_1^2 - 4A_2A_0}) < 0$ , for which  $v_1 = 0$ , and then we apply the Groebner basis reduction method (under the condition  $v_1 = 0$ ) to obtain

$$v_2|_{v_1=0} = -\frac{C}{96D^2(1-X_2)^2(X_2+D)^2(1+D-X_2)^2} \left\{ -E^-(1-X_2)^2(1+D-X_2)^2[3(1-2X_2)^3 + (1+D)(7(1+2D) + 4(1-2X_2)(2+7D+10X_2))] + D(1-2X_2) \right. \\ \times \left[ \frac{3}{4}(1-2X_2)^4 + 4(7+4D)X_2^3 + \frac{1}{4}(57+94D+52D^2)(1-4X_2^2) \right. \\ \left. \left. + (1-2X_2)(3+36D+58D^2+28D^3) + \frac{1}{2}D(31+56D+28D^2) \right] \right\} < 0,$$

due to  $X_2 \in (0, \frac{1}{2})$ , indicating that bifurcation of three small-amplitude limit cycles are not possible from a Hopf critical point. Thus, for Case (iiib), two small-amplitude limit cycles can bifurcate from the Hopf critical point near  $E_2^-$ , and the outer one is stable while the inner one is unstable, both of them enclosing the stable equilibrium  $E_2^-$ . This shows that the codimension of the (generalized) Hopf bifurcation is two. The number of the sets of parameter values to generate two limit cycles can also be infinite. It should be noted that when  $\tilde{C} = \tilde{C}^- < 0$ , we have  $C = C^* - \tilde{C}^- > 0$  and can show that  $-2\sqrt{A} < B = \frac{2}{D}(1-X_2)E^- < 0$ . For example, we again choose  $D = 1$  and  $X_2 = \frac{1}{4}$ , and then use (35), (44) and (45) to obtain other parameter values, given below:

$$A = \frac{16}{21609}(847 + 31\sqrt{769}), \\ B = -\frac{4}{147}(13 + \sqrt{769}), \tag{47}$$

which indeed yield

$$C - AD = -\frac{8}{21609}(371 + 13\sqrt{769}) < 0, \\ B + 2\sqrt{A} = \frac{-4(13 + \sqrt{769}) + 8\sqrt{847 + 31\sqrt{769}}}{147} \\ \approx 1.139933 > 0,$$

as required. Further, the focus values become

$$\tilde{C} = \tilde{C}^- = -\frac{8}{441}(13 + \sqrt{769}), \\ C = C^* - \tilde{C} = \frac{8}{441}(27 + \sqrt{769}),$$

$$v_0 = v_1 = 0, \\ v_2 = -\frac{16}{14586075}(268349 + 9677\sqrt{769}) < 0,$$

showing that the outer limit cycle is stable.

It has been noted that in both cases, the outer limit cycle is stable. When  $B \geq 0$ , the unique limit cycle is stable and the enclosed equilibrium  $E_2^-$  is unstable; when  $B < 0$ , the equilibrium becomes stable and the second unstable limit cycle emerges between the stable equilibrium and the outer stable limit cycle. This indicates that the dynamical behavior of the model outside the limit cycle(s) is unchanged, see Figs. 8 and 9 in the next section.

This completes the proof of Theorem 3.1. ■

### 4. Simulation

In this section, we present simulations to demonstrate the existence of one and two limit cycles in the  $B_{iii}$  model. We apply a fourth-order Runge–Kutta numerical integration method implemented on a PC machine. Two sets of numerical examples are given in (46) and (47), yielding one and two limit cycles for cases  $B \geq 0$  and  $B < 0$ , respectively.

First, consider the parameter values given in (46) for the case  $B \geq 0$ , yielding one limit cycle. For this set of parameter values, since  $v_1 = -\frac{5413}{144506880} \approx -0.0000375$ , we need to perturb the parameter values such that  $0 < v_0 \ll |v_1|$ . We choose the values of  $A$  and  $B$  from (46) but take perturbation on  $C$  as

$$C = \frac{1}{126} + \varepsilon \approx 0.007987, \quad \text{where } \varepsilon = 0.5 \times 10^{-4},$$

for which the focus values  $v_0$  and  $v_1$  become  $v_0 = 0.269481 \times 10^{-5}$  and  $v_1 = -355904 \times 10^{-4}$ . Then, the truncated normal form equation  $v_0 + v_1 r^2 = 0$  gives a positive root  $r_1 = 0.275168$ , which approximates the amplitude of the stable limit cycle, confirmed by the simulation shown in Fig. 8, where the four equilibria are  $E_0 : (0, 0)$ ,  $E_1 : (1, 0)$ ,  $E_2^- : (0.249983, 0.001488)$ , and  $E_2^+ : (8.250017, -18.093763)$  which has no biological meaning. For this case, since both  $E_0$  and  $E_1$  are saddle points, and  $E_2^-$  is an unstable focus, bistable phenomenon does not exist.

Next, consider the parameter values given in (47) for the case  $B < 0$ , giving two limit cycles. This example belongs to the Case (iiib), since

$$A = \frac{16}{21609}(847 + 31\sqrt{769}),$$

$$B = -\frac{4}{147}(13 + \sqrt{769}) < 0$$

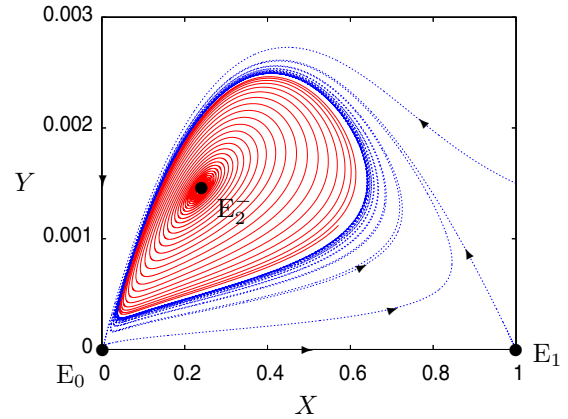


Fig. 8. Simulated phase portrait for the  $B_{iii}$  model (14) with  $A = 0.00570437$ ,  $B = 0.36904762$ ,  $C = 0.00798651$ ,  $D = 1$ , showing one limit cycle without bistable phenomenon.

and so  $B + 2\sqrt{A} \approx 1.139933202 > 0$  for which we indeed have  $C \approx 0.9928498731 > C_1 \approx 0.2539682540$ .

Further, we take the following perturbations:

$$C = \frac{8}{441}(27 + \sqrt{769}) + \varepsilon_1,$$

$$A = \frac{16}{21609}(847 + 31\sqrt{769}) - \varepsilon_2,$$

where  $\varepsilon_1 = 0.001$ ,  $\varepsilon_2 = 0.000000005$ , under which the focus values become

$$v_0 \approx -0.5 \times 10^{-8}, \quad v_1 \approx 0.00022631,$$

$$v_2 \approx -0.71726168.$$

So the equation  $v_0 + v_1 r^2 + v_2 r^4 = 0$  gives two positive solutions:  $r_1 = 0.004889$ ,  $r_2 = 0.017077$ , which approximate the amplitudes of the two bifurcating limit cycles. Note that  $v_0 < 0$  and  $v_2 < 0$  indicate that the equilibrium  $E_2^-$  and the outer limit cycle are stable, while the inner limit cycle is unstable since  $v_1 > 0$ . Also note that the absolute value of  $v_0$  is very small, it is expected that the convergence speed of the trajectories to the equilibrium  $E_2^-$  is very slow.

The simulations are shown in Fig. 9. Figure 9(a) depicts the four equilibria:  $E_0 : (0, 0)$ ,  $E_1 : (1, 0)$ ,  $E_2^- : (0.25, 0.18635)$  and  $E_2^+ : (0.63331, 0.23080)$ . Indeed,  $E_0$  and  $E_2^+$  are saddle points,  $E_1$  is a stable node, and  $E_2^-$  is a stable focus. [Trajectories converging to the equilibrium  $E_2^-$  are not shown in Fig. 9(a) because the trapping area is too small.] In Fig. 9(b), we show the two limit cycles. The convergence of the large stable limit cycle is pretty fast.

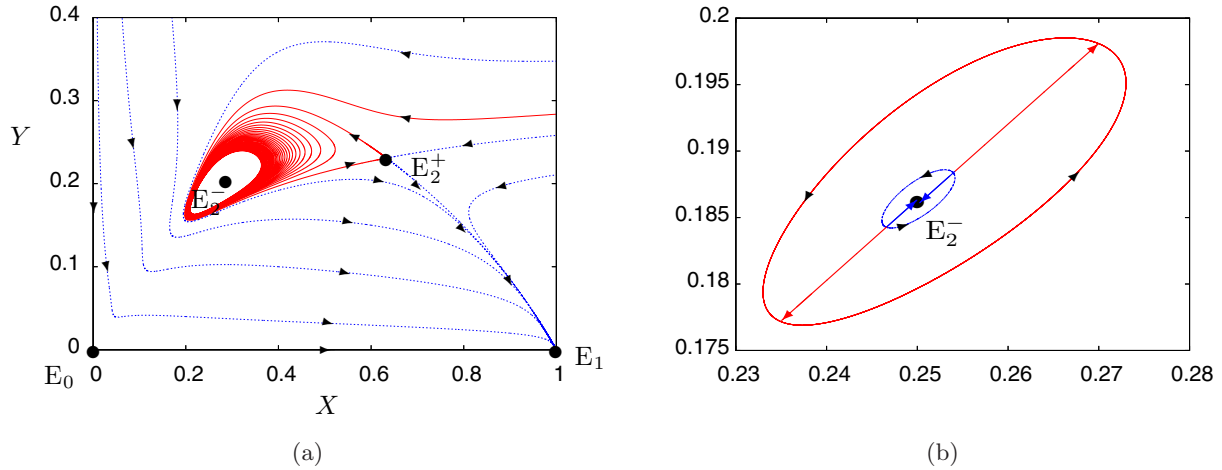


Fig. 9. Simulated phase portraits for system  $B_{iii}$  (14) with  $A = 1.26549514$ ,  $B = -1.10982243$ ,  $C = 0.99384987$ ,  $D = 1$ , showing two limit cycles: (a) trajectories converging to the equilibrium  $E_1$  or the large limit cycle and (b) two limit cycles with the outer being stable and inner being unstable, where the arrows indicate the moving direction of solution trajectories.

We do not show the nearby trajectories converging to the limit cycle but just the two limit cycles for a clear view, with the red arrows to indicate the trajectories moving towards the stable large limit cycle and the blue arrow to indicate the trajectories moving towards the stable equilibrium, and an unstable small limit cycle (in blue color) between them. It is seen that this simulated stable limit cycle agrees well with the analytical prediction.

For the small unstable limit cycle, we use the so-called time-reversible numerical integration scheme, that is, merely taking negative time steps in the numerical integration approach. This technique changes  $\alpha$ -limit sets to  $\omega$ -limit sets and thus unstable limit cycles become “stable”. It should be noted that this time-reversible integration technique does not work for dynamical systems with dimension higher than two. Due to the very small absolute values of  $v_0$ , the convergence speed of trajectories to the unstable limit cycle from inside is extremely slow, but they agree well with the analytical prediction.

This example shows an interesting *tristable phenomenon*, that is, the system can simultaneously have two equilibria,  $E_1$ ,  $E_2^-$ , and a stable limit cycle. Depending on initial conditions, trajectories may converge to the stable equilibrium  $E_1$ , or the equilibrium  $E_2^-$ , or the stable limit cycle. The saddle separatrixes connecting the equilibrium  $E_2^+$  [i.e. a half-stable trajectory converging to this point and a half-unstable trajectory diverging from this point, see Fig. 9(a)] separate the trapping regions of  $E_1$  and the stable limit cycle. The trapping region of

the stable limit cycle is inside the saddle separatrixes and the unstable limit cycle. The trapping region of the equilibrium  $E_2^-$  is the area inside the unstable limit cycle. In other words, the unstable limit cycle is a separator for the equilibrium  $E_2^-$  and the stable limit cycle. It should be noted that the trapping region of the equilibrium  $E_2^-$  is small, and most of trajectories converge either to the stable node  $E_1$  or the stable limit cycle.

## 5. Conclusion

In this paper, we present a detailed study on a predator–prey system with Holling type III ratio-dependent functional response. Explicit conditions on parameters are given to classify various bifurcations. In particular, it is proved that one or two Hopf bifurcations occur from the epidemic equilibrium. Moreover, multiple limit cycles bifurcation analysis is carried out to show that maximal one limit cycle occurs from a Hopf critical point when  $B \geq 0$ , and maximal two limit cycles occur from a Hopf critical point when  $B < 0$ . The bifurcation of two limit cycles yields tristable phenomenon, demonstrating complex dynamical behavior in predator–prey systems. The method presented in this paper can be applied to study other biological and physical systems.

## Acknowledgments

This research was partially supported by the National Natural Science Foundation of China (No. 11201294), the Innovation Program of Shanghai

Municipal Education Commission (No. 14YZ114), and the Natural Sciences and Engineering Research Council of Canada (No. R2686A02).

## References

- Andrews, J. F. [1968] "A mathematical model for the continuous culture of microorganisms utilizing inhibitory substrates," *Biotechnol. Bioeng.* **10**, 707–723.
- Arditi, R. & Ginzburg, L. R. [1989] "Coupling in predator–prey dynamics: Ratio dependence," *J. Theor. Biol.* **139**, 311–326.
- Arditi, R., Ginzburg, L. R. & Akcakaya, H. R. [1991] "Variation in plankton densities among lakes: A case for ratio-dependent models," *Am. Nat.* **138**, 1287–1296.
- Arditi, R. & Saiah, H. [1992] "Empirical evidence of the role of heterogeneity in ratio-dependent consumption," *Ecology* **73**, 1544–1551.
- Bazykin, A. D. [1998] *Nonlinear Dynamics of Interaction Populations*, World Sci. Ser. Nonlin. Sci. Ser. A, Vol. 11 (World Scientific, Singapore).
- Beddington, J. R. [1975] "Mutual interference between parasites or predators and its effect on searching efficiency," *J. Anim. Ecol.* **44**, 331–340.
- Berezovskaya, F., Karev, G. & Arditi, R. [2001] "Parametric analysis of the ratio-dependent predator–prey model," *J. Math. Biol.* **43**, 221–246.
- Berryman, A. A. [1992] "The origin and evolution of predator–prey theory," *Ecology* **73**, 1530–1535.
- Bishop, M. J., Kelaher, B. P., Smith, M., York, P. H. & Booth, D. J. [2006] "Ratio-dependent response of a temperate Australian estuarine system to sustained nitrogen loading," *Oecologia* **149**, 701–708.
- Boon, B. & Landelout, H. [1962] "Kinetics of nitrite oxidation by nitrobacter winogradski," *Biochem. J.* **85**, 440–447.
- Broer, H., Saleh, K., Naudot, V. & Roussarie, R. [2006] "Dynamics of a predator–prey model with non-monotonic response function," *Regul. Chaot. Dyn.* **11**, 155–165.
- Chow, S. N., Li, C. C. & Wang, D. [1994] *Normal Forms and Bifurcation of Planar Vector Fields* (Cambridge University Press, Cambridge).
- Collings, J. B. [1997] "The effects of the functional response on the behavior of a mite predator–prey interaction model," *J. Math. Biol.* **36**, 149–168.
- Cosner, C., DeAngelis, D. L., Ault, J. S. & Olson, D. B. [1999] "Effects of spatial grouping on the functional response of predators," *Theor. Popul. Biol.* **56**, 65–75.
- Dai, Y., Zhao, Y. & Sang, B. [2019] "Four limit cycles in a predator–prey system of Leslie type with generalized Holling type III functional response," *Nonlin. Anal.: Real World Appl.* **50**, 218–239.
- DeAngelis, D. L., Goldstein, R. A. & O'Neill, R. V. [1975] "A model for trophic interactions," *Ecology* **56**, 881–892.
- Edwards, V. H. [1970] "Influence of high substrate concentrations on microbial kinetics," *Biotechnol. Bioeng.* **12**, 679–712.
- Fenichel, N. [1979] "Geometric singular perturbation theory for ordinary differential equations," *J. Diff. Eqs.* **31**, 53–98.
- Freedman, H. I. [1980] *Deterministic Mathematical Models in Population Ecology* (Marcel Dekker, NY).
- Gause, G. F. [1969] *The Struggle for Existence*, (Hafner Publishing Company, NY).
- Gazor, M. & Yu, P. [2012] "Spectral sequences and parametric normal forms," *J. Diff. Eqs.* **252**, 1003–1031.
- Guckenheimer, J. & Holmes, P. [1993] *Nonlinear Oscillations, Dynamical Systems, and Bifurcations of Vector Fields*, 4th edition (Springer, NY).
- Gutierrez, A. P. [1992] "The physiological basis of ratio-dependent predator–prey theory: A metabolic pool model of Nicholson's blowflies as an example," *Ecology* **73**, 1552–1563.
- Han, M. & Yu, P. [2012] *Normal Forms, Melnikov Functions, and Bifurcations of Limit Cycles* (Springer, NY).
- Hanski, I. [1991] "The functional response of predators: Worries about scale," *Trends Ecol. Evol.* **6**, 141–142.
- Haque, M. [2009] "Ratio-dependent predator–prey models of interacting populations," *Bull. Math. Biol.* **71**, 430–452.
- Holling, C. S. [1959a] "The components of predation as revealed by a study of small-mammal predation of the European pine sawfly," *Can. Entomol.* **91**, 293–320.
- Holling, C. S. [1959b] "Some characteristics of simple types of predation and parasitism," *Can. Entomol.* **91**, 385–398.
- Holling, C. S. [1965] "The functional response of predator to prey density and its role in mimicry and population regulation," *Mem. Entomol. Soc. Can.* **97**, 5–60.
- Hsu, S. B., Hwang, T. W. & Kuang, Y. [2001] "Global analysis of the Michaelis–Menten type ratio-dependent predator–prey system," *J. Math. Biol.* **42**, 489–506.
- Huang, J., Ruan, S. & Song, J. [2014] "Bifurcations in a predator–prey system of Leslie type with generalized Holling type III functional response," *J. Diff. Eqs.* **257**, 1721–1752.
- Jiang, J. & Yu, P. [2017] "Multistable phenomena involving equilibria and periodic motions in predator–prey systems," *Int. J. Bifurcation and Chaos* **27**, 1750043–1–18.
- Jost, J. L., Drake, J. F., Fredrickson, A. G. & Tsuchiya, H. M. [1973a] "Interactions of tetrahymena pyriformis, escherichia coli, azotobacter vinelandii, and glucose in a minimal medium," *J. Bacteriol.* **113**, 834–840.

- Jost, J. L., Drake, J. F., Tsuchiya, H. M. & Fredrickson, A. G. [1973b] “Microbial food chains and food webs,” *J. Theor. Biol.* **41**, 461–484.
- Jost, C., Arino, O. & Arditi, R. [1999] “About deterministic extinction in ratio-dependent predator–prey model,” *Bull. Math. Biol.* **61**, 19–32.
- Kuang, Y. & Freedman, H. I. [1988] “Uniqueness of limit cycles in Gause type models of predator–prey systems,” *Math. Biosci.* **88**, 67–84.
- Kuang, Y. & Beretta, E. [1998] “Global qualitative analysis of a ratio-dependent predator–prey system,” *J. Math. Biol.* **36**, 389–406.
- Kuang, Y. [1999] “Rich dynamics of Gause-type ratio-dependent predator–prey systems,” *Fields Inst. Commun.* **21**, 325–337.
- Kuznetsov, Y. A. [1998] *Elements of Applied Bifurcation Theory*, 2nd edition (Springer, NY).
- Lamontagne, Y., Coutu, C. & Rousseau, C. [2008] “Bifurcation analysis of a predator–prey system with generalised Holling type III function response,” *J. Dyn. Diff. Eqs.* **20**, 535–571.
- Li, B. & Kuang, Y. [2007] “Heteroclinic bifurcation in the Michaelis–Menten type ratio-dependent predator–prey system,” *SIAM J. Appl. Math.* **67**, 1453–1464.
- Lotka, A. [1925] *Elements of Physical Biology* (Williams and Wilkins, Baltimore).
- May, R. M. [1973] *Stability and Complexity in Model Ecosystems*, Princeton University Press (Princeton, NJ).
- Morozov, A. Y. & Arashkevich, A. G. [2008] “Patterns of zooplankton functional response in communities with vertical heterogeneity: A model study,” *Math. Model. Nat. Phenom.* **3**, 131–148.
- Murray, J. D. [2002] *Mathematical Biology (II)* (Springer-Verlag, Berlin, Heidelberg).
- Pal, P. J., Mandal, P. K. & Lahiri, K. K. [2014] “A delayed ratio-dependent predator–prey model of interacting populations with Holling type III functional response,” *Nonlin. Dyn.* **76**, 201–220.
- Reeve, J. D. [1997] “Predation and bark beetle dynamics,” *Oecologia* **112**, 48–54.
- Ruan, S. & Xiao, D. [2001] “Global analysis in a predator–prey system with nonmonotonic functional response,” *SIAM J. Appl. Math.* **61**, 1445–1472.
- Seo, G. & DeAngelis, D. L. [2011] “A predator–prey model with a Holling type I functional response including a predator mutual interference,” *J. Nonlin. Sci.* **21**, 811–833.
- Solomon, M. E. [1949] “The natural control of animal populations,” *J. Anim. Ecol.* **18**, 1–35.
- Taylor, R. J. [1984] *Predation* (Chapman and Hall, NY).
- Tian, Y. & Yu, P. [2013] “An explicit recursive formula for computing the normal form and center manifold of  $n$ -dimensional differential systems associated with Hopf bifurcation,” *Int. J. Bifurcation and Chaos* **23**, 1350104-1–18.
- Tian, Y. & Yu, P. [2014] “An explicit recursive formula for computing the normal forms associated with semisimple cases,” *Commun. Nonlin. Sci. Numer. Simul.* **19**, 2294–2308.
- Volterra, V. [1926] “Fluctuations in the abundance of species considered mathematically,” *Nature* **118**, 558–560.
- Wang, C. & Zhang, X. [2019] “Canards, heteroclinic and homoclinic orbits for a slow–fast predator–prey model of generalized Holling type III,” *J. Diff. Eqs.* **267**, 3397–3441.
- Xiao, D. & Ruan, S. [2001] “Global dynamics of a ratio-dependent predator–prey system,” *J. Math. Biol.* **43**, 268–290.
- Xiao, D., Li, W. & Han, M. [2006] “Dynamics in a ratio-dependent predator–prey model with predator harvesting,” *J. Math. Anal. Appl.* **324**, 14–29.
- Xu, R., Gan, Q. & Ma, Z. [2009] “Stability and bifurcation analysis on a ratio-dependent predator–prey model with time delay,” *J. Comput. Appl. Math.* **230**, 187–203.
- Yu, P. [1998] “Computation of normal forms via a perturbation technique,” *J. Sound Vibr.* **211**, 19–38.
- Yu, P. & Leung, A. Y. T. [2003] “The simplest normal form of Hopf bifurcation,” *Nonlinearity* **16**, 277–300.
- Yu, P. & Han, M. [2005] “Small limit cycles bifurcating from fine focus points in cubic-order  $Z_2$ -equivariant vector fields,” *Chaos Solit. Fract.* **24**, 329–348.